Geophys. Astrophys. Fluid Dynamics, 1980, Vol. 15, pp. 167–211
0309-1929/80/1504-0167 $06.50/0
© Gordon and Breach Science Publishers Inc., 1980
Printed in Great Britain

Baroclinic Instability and Geostrophic Turbulence

RICK SALMON

Scripps Institution of Oceanography (A-025), La Jolla, California 92093, U.S.A.

(*Received November 15, 1979*)

I examine the geostrophic turbulence field in equilibrium with a horizontally uniform mean zonal flow driven by solar heating. The equilibrium mean vertical shear is highly supercritical, and the turbulence field has its maximum in kinetic energy at wavenumbers smaller than the wavenumbers of fastest growth predicted by linear stability theory. Wavenumber spectra obtained by averaging lengthy numerical integrations of the two-level quasi-geostrophic equations agree well with the predictions of a simple Markovian turbulence model. Analysis of the turbulence model suggests that the most energetic wavenumbers equilibrate from scattering of the temperature perturbations into higher wavenumbers by the barotropic advecting field. In the higher unstable wavenumbers, including the most supercritical, linear instability is offset chiefly by local rotations of the unstable structures by larger, more energetic eddies.

1. INTRODUCTION

The general circulation of the atmosphere and more particularly the growth and decay of baroclinic waves fueled by potential energy in the zonally averaged flow have been studied for many years. Most previous theoretical studies have employed small amplitude expansions of the flow field about a zonal mean current. While these theories have proved physically insightful, and are apparently adequate to explain many features of the observed finite-amplitude flow, they may be incapable of detailing the physical processes that ultimately limit the growth of unstable waves and bring about a statistically steady final state. The establishment of such state clearly depends on nonlinear effects.

Highly nonlinear flow is the province of direct numerical simulations of the equations of motion, and statistical turbulence theory. In contrast to the linear perturbation theory, which is an expansion about a state of small amplitude, the turbulence theories of the "direct-interaction family"

may be looked on as expansions about a completely random state. The turbulence theories make no unrealistic assumptions about the amplitude of the motion.

This paper studies the highly nonlinear geostrophic turbulence field that arises on a horizontally uniform mean zonal flow with vertical shear. The phrase "finite-amplitude baroclinic instability" aptly describes the geometry and physics. The tools of the analysis are elementary physical reasoning, direct simulations of the two-level quasi-geostrophic equations of motion, a closure theory of turbulence, and related simple ideas from statistical mechanics. The primary goal is to explain the mechanism by which amplifying baroclinic waves reach statistical equilibrium in a simple atmospheric model, and to examine the nature of the equilibrium state.

In a previous study (Salmon, 1978; hereinafter called S78) I considered two-layer quasi-geostrophic turbulence under the simplifying assumptions of horizontal isotropy and uniform vertical average energy density. The former study offered physical insight, but the imposed statistical symmetry proved too severe to permit detailed comparison between the theory and geophysical observations. The present study replaces the isotropic stirring force of S78 by a westerly mean flow with vertical shear. The mean shear is maintained by solar heating, and it is the source of energy for the turbulence field, which is of central interest. The mean flow is constrained to be horizontally uniform so that the turbulence field is statistically homogeneous in the horizontal, but anisotropy induced by the mean flow and by the earth's curvature (the beta-effect) is now included in the theory. Also unlike S78, the present study uses Ekman friction at the lower boundary only. The qualitative arguments of S78 (which are summarized below but not reproduced in detail) apply fully to the new model, but I am here primarily concerned with those new features of the turbulence that depend on the presence of the mean flow and the beta-effect. However, this paper should be read as a sequel to S78.

I have tried to present my results in a way which would appeal both to meteorologists and turbulence theorists. Section 2 describes the model equations of motion and reviews important features of the baroclinic instability problem. Section 3 extends the qualitative theory of S78 and proposes several testable mechanisms for baroclinic adjustment. Section 4 reports three lengthy numerical simulations with differing values of beta and ground friction. Section 5 describes the turbulence closure. Readers who are unfamiliar with closure methods can skip Section 5 with little loss in continuity. Section 6 compares the wavenumber spectra predicted by closure with the results of the numerical simulations. The agreement is good. Close inspection of the closure equation governing northward heat flux reveals the fundamental result of the paper: that linear instability is

ultimately limited by the scrambling effect of larger-scale barotropic motions. This observation suggests an asymptotic analysis, pursued in Section 7, in which the scrambling mechanism is related more specifically (but with less quantitative confidence) to stretchings and rotations of a passively advected wavevector which represents the heat flux in unstable eddies.

In many previous applications, turbulence closure theories have been used to extend the resolution (or Reynold's number) attainable by direct simulation of the equations of motion. In this paper both the closure and simulation experiments are performed at a relatively low resolution corresponding to a square with 32 gridpoints in each direction. The low resolution permits the simulations to be integrated long enough to get stable averages of the large scales of motion, and finer resolution is perhaps not justified by the quasi-geostrophic dynamics. Here, the closure is used primarily to compute the effects of one *statistic* on another in a way that permits analytical simplifications after the dominant terms are identified. As in S78, the primary goal is physical insight.

2. THE MODEL

The model equations are nearly the same as those used in S78, except that now a strictly meteorological interpretation is placed on all variables. The dependent variables are ψ_1, the streamfunction for the horizontal velocity at the upper (nominal 250 mb) level; and ψ_2, the streamfunction at the lower (750 mb) level. The governing quasi-geostrophic vorticity equations at the two levels are

$$\frac{\partial \zeta_i}{\partial t} + J(\psi_i, \zeta_i) = F_i, \quad i = 1, 2 \tag{2.1a}$$

where

$$\zeta_i = \nabla^2 \psi_i + f + \tfrac{1}{2} k_R^2 (\psi_j - \psi_i), \quad j = 3 - i \tag{2.1b}$$

and

$$J(a, b) = \frac{\partial a}{\partial x}\frac{\partial b}{\partial y} - \frac{\partial b}{\partial x}\frac{\partial a}{\partial y}. \tag{2.1c}$$

In the above equations, F_i is the frictional torque at the ith level; k_R^{-1} (units of length) is the internal Rossby deformation radius; and f is twice the local vertical component of the earth's rotation. The Cartesian coordinates (x, y) measure distance in the (east, north) direction. Vertical dependence has been removed by finite differencing, and the differencing incorporates the vertical boundary conditions of no vertical motion at

0 mb and at the earth's surface (in the case of no viscosity). The Coriolis parameter f is prescribed by

$$f = f_0 + \beta y, \tag{2.2}$$

where f_0 and β are constants. Equations (2.1–2.2) are standard in meteorology (Rossby, 1939; Charney and Phillips, 1952). For a discussion, see Haltiner (1966). For a modern derivation, see Pedlosky (1964).

In this paper, I set

$$\psi_1 = -V_1 y + \psi_1', \quad \text{and} \quad \psi_2 = -V_2 y + \psi_2', \tag{2.3}$$

where V_1 and V_2 are either prescribed constants or vary only in time as described below. The primed streamfunctions ψ_1', ψ_2' are constrained to be periodic in x and y with period L_p. The periodic box has the same surface area as earth, that is

$$L_p^2 = 4\pi r_e^2, \tag{2.4}$$

where r_e is the radius of the earth. The westerly mean flow (V_1, V_2) is the sole source of energy for the periodic motion. However, only the difference $V_1 - V_2$ is dynamically relevant, since the effect of a completely uniform mean current can be removed from the equations by Galilean transformation. For this reason I take

$$V_1 = -V_2 = V \tag{2.5}$$

in (2.3). The frictional torques F_i are given to be

$$F_1 = 0, \quad \text{and} \quad F_2 = -\lambda \nabla^2 \psi_s, \tag{2.6}$$

where λ is the coefficient of (Ekman) friction with the earth's surface and ψ_s is the streamfunction at the surface.

In place of ψ_1', ψ_2' it is convenient to work with the modal variables

$$\psi = \tfrac{1}{2}(\psi_1' + \psi_2'), \quad \text{and} \quad \tau = \tfrac{1}{2}(\psi_1' - \psi_2'). \tag{2.7}$$

The "barotropic" streamfunction ψ may be regarded as the streamfunction at 500 mb. The "baroclinic" streamfunction τ is proportional to the 500 mb temperature. In terms of ψ, τ (2.1) become

$$\nabla^2 \psi_t + \beta \frac{\partial \psi}{\partial x} + V \frac{\partial}{\partial x} \nabla^2 \tau + J(\psi, \nabla^2 \psi) + J(\tau, \nabla^2 \tau) + \frac{\lambda}{2} \nabla^2 \psi_s = 0, \tag{2.8}$$

and

$$\nabla^2\tau_t+\beta\frac{\partial\tau}{\partial x}+V\frac{\partial}{\partial x}\nabla^2\psi+J(\psi,\nabla^2\tau)+J(\tau,\nabla^2\psi)-\frac{\lambda}{2}\nabla^2\psi_s$$
$$=k_R^2\left[\tau_t-V\frac{\partial\psi}{\partial x}+J(\psi,\tau)\right], \qquad (2.9)$$

which are closed by setting

$$\psi_s=\psi-1.6\tau. \qquad (2.10)$$

The factor of 1.6 comes from linear extrapolation with height through a "standard atmosphere".

If $V=\lambda=0$, then (2.8, 2.9) conserve the mechanical energy of the periodic flow, defined (in units of energy per unit area) as

$$E=\frac{\Delta p}{2g}[\nabla\psi_1'\cdot\nabla\psi_1'+\nabla\psi_2'\cdot\nabla\psi_2'+\tfrac{1}{2}k_R^2(\psi_1'-\psi_2')^2]_{\text{area}}$$
$$=\frac{\Delta p}{g}[\nabla\psi\cdot\nabla\psi+\nabla\tau\cdot\nabla\tau+k_R^2\tau^2]_{\text{area}} \qquad (2.11)$$

where

$$\Delta p=500\,\text{mb} \quad \text{and} \quad g=9.8\,\text{m sec}^{-2},$$

and the square brackets denote average over the periodic box. The three terms on the right side of (2.11a) represent the kinetic energy in the top layer, the kinetic energy in the bottom layer, and the available potential energy. The three terms in (2.11b) represent the kinetic energy in barotropic flow, baroclinic kinetic energy, and the available potential energy.

If $V\neq0$, the rate of production (per unit area) of energy in periodic flow from the mean flow energy is

$$P=(2Vk_R^2\Delta p/g)[\psi_x\tau]_{\text{area}} \qquad (2.12)$$

which is proportional to the northward eddy heat flux at 500 mb.

A well-known stability calculation examines the behavior of (2.8, 2.9) when the periodic motion is weak enough so that V may be considered constant and the nonlinear terms in ψ, τ neglected. With $\lambda=0$ (for simplicity) one finds solutions of the form real part of

$$\psi=\text{const}\cdot\exp[i(k_x x+k_y y-\omega t)] \qquad (2.13)$$

and

$$\tau = (\omega + \beta k_x/k^2)\psi/Vk_x,$$

where

$$\omega = \frac{-\beta k_x}{(k^2+k_R^2)}\left[1+\frac{k_R^2}{2k^2} \pm \frac{k_R^2}{2k^2}\left(1+\frac{4k^4(k^4-k_R^4)}{k_\beta^4 k_R^4}\right)^{1/2}\right], \tag{2.14}$$

$$k^2 \equiv k_x^2 + k_y^2, \quad \text{and} \quad k_\beta^2 \equiv \beta/V.$$

For $\beta = 0$, (2.14) reduces to

$$\omega = \pm Vk_x\left(\frac{k^2-k_R^2}{k^2+k_R^2}\right)^{1/2}, \tag{2.15}$$

and all wavenumbers **k** (with $k_x \neq 0$) on $k < k_R$ are unstable. Fastest growth occurs for $k = k_x = 0.644\, k_R$. By (2.13) the 500 mb temperature field is displaced ninety degrees west in phase from the streamfunction ψ in all growing waves. This corresponds to optimal correlation between warm and north-flowing air to maintain instability. If $\beta \neq 0$ but $k_\beta < k_R$, then at least some of the wavenumbers **k** on $k < k_R$ are unstable. Under typical midlatitude conditions, $k_\beta \sim 4$, $k_R \sim 8$, and the unstable range extends approximately from $k_\beta/2^{1/2}$ to k_R.† The phase lag between ψ and τ is reduced from the optimum value at all k, and growth rates are less than with $\beta = 0$. All of these unstable modes are "deep" in the sense of Held (1978). If $V = 0$, (2.14) reduces to the dispersion relation for barotropic and baroclinic Rossby waves,

$$\omega = \begin{cases} -\beta k_x/k^2; & \psi \neq 0, \quad \tau = 0, \\ -\beta k_x/(k^2+k_R^2); & \psi = 0, \quad \tau \neq 0. \end{cases} \tag{2.16}$$

The baroclinic instability calculation has, of course, been made on numerous more sophisticated dynamical models using more realistic mean flow profiles. However, many workers have noted that, in some respects, the calculations on simple models like the one used here compare better with atmospheric observations than do the more refined calculations. Smagorinsky (1963), Moura and Stone (1976) and especially Stone (1978) present evidence that the observed zonal shear is near the critical value predicted by the two-level model at latitudes from 40–45°N to 75°N, in all four seasons.

†All quantities in this paper will have dimensional values, to facilitate comparison with real data. The single exception will be wavenumbers, which will always be given in nondimensional form. The convention is that "wavenumber n" has n cycles in a distance L_p.

The statistical theory introduced in Section 5 provides a closed set of equations in the second moments (the wavenumber spectra) of ψ and τ. The remaining task of this section is to deduce the form these moments can take. Let the streamfunctions be expanded in Fourier series,

$$\psi^n(\mathbf{x},t)=\sum_{\mathbf{k}}\psi^n_{\mathbf{k}}(t)e^{i\mathbf{k}\cdot\mathbf{x}} \tag{2.17}$$

where

$$\psi^n\equiv\begin{cases}\psi, & \text{if} \quad n=0\\ \tau, & \text{if} \quad n=1,\end{cases}$$

and $\mathbf{x}$ is horizontal position. Since ψ^n is real, $\psi^n_{\mathbf{k}}$ is conjugate symmetric. Let $\langle\ \rangle$ denote ensemble average. Since the flow is statistically homogeneous in $\mathbf{x}$, the only nonvanishing spectral moments are of the form

$$R^{ij}_{\mathbf{k}}=\langle\psi^i_{\mathbf{k}}\psi^j_{-\mathbf{k}}\rangle. \tag{2.18}$$

By conjugate symmetry of $\psi^i_{\mathbf{k}}$,

$$R^{ij}_{\mathbf{k}}=(R^{ji}_{\mathbf{k}})^*, \tag{2.19}$$

and by a symmetry property of the model equations,†

$$R^{ij}_{(k_x,k_y)}=R^{ij}_{(k_x,-k_y)}. \tag{2.20}$$

Define

$$\begin{gathered}U(\mathbf{k})\equiv k^2\langle\psi_{\mathbf{k}}\psi_{-\mathbf{k}}\rangle/|d\mathbf{k}|, \quad T(\mathbf{k})\equiv k^2\langle\tau_{\mathbf{k}}\tau_{-\mathbf{k}}\rangle/|d\mathbf{k}|,\\ D(\mathbf{k})\equiv k^2\,\text{Real}\,\langle\psi_{\mathbf{k}}\tau_{-\mathbf{k}}\rangle/|d\mathbf{k}|, \quad F(\mathbf{k})\equiv -k^2\,\text{Imag}\,\langle\psi_{\mathbf{k}}\tau_{-\mathbf{k}}\rangle/|d\mathbf{k}|\end{gathered} \tag{2.21}$$

and

$$E(\mathbf{k})\equiv(k^2+k_R^2)T(\mathbf{k})/k^2,$$

and let

$$k\equiv k(\cos\theta,\sin\theta),$$

where θ is the angle measured counterclockwise to $\mathbf{k}$ from the k_x-axis. It follows from (2.19) and (2.20) that the spectra may be expanded in angular series of the general forms

$$U(\mathbf{k})=U(k)\left[1+\sum_{n=1}^{\infty}U_{2n}(k)\cos(2n\theta)\right], \tag{2.22}$$

†If $\psi(x,y)$ and $\tau(x,y)$ solve (2.8, 2.9) then so do $-\psi(x,-y)$ and $-\tau(x,-y)$. If the ensemble of initial conditions contains both solutions with equal probability then (2.20) holds for all time.

plus corresponding equations with U replaced by T and then D; and

$$F(\mathbf{k})=F(k)\cos\theta+\sum_{n=1}^{\infty}F_{2n+1}(k)\cos[(2n+1)\theta]. \tag{2.23}$$

It is convenient to define

$$\begin{aligned}&\bar{U}(k)=2\pi kU(k),\quad \bar{T}(k)=2\pi kT(k),\quad \bar{D}(k)=2\pi kD(k),\\ &\bar{F}(k)=2\pi k_R^2\langle V\rangle F(k),\quad \bar{E}(k)=(k^2+k_R^2)k^{-2}\bar{T}(k).\end{aligned} \tag{2.24}$$

The physical content of these spectra can best be learned by inspecting the statement

$$\text{Quantity}=\frac{\Delta p}{g}\int_0^{\infty}(\text{Integrand})dk,$$

with the various substitutions from Table I. In summary, positive $U_2(k)(T_2(k))$ corresponds to elongation of barotropic (baroclinic) eddies

TABLE I

Quantity	Integrand
Barotropic energy	$\bar{U}(k)$
Baroclinic kinetic energy	$\bar{T}(k)$
Total kinetic energy	$\bar{U}(k)+\bar{T}(k)$
Available potential energy	$k_R^2\bar{T}(k)/k^2$
Total baroclinic energy	$\bar{E}(k)$
Total energy	$\bar{U}(k)+\bar{E}(k)$
Kinetic energy in the upper layer	$\frac{1}{2}[\bar{U}(k)+\bar{T}(k)+2\bar{D}(k)]$
Kinetic energy in the lower layer	$\frac{1}{2}[\bar{U}(k)+\bar{T}(k)-2\bar{D}(k)]$
Production of turbulent energy from the mean flow	$\bar{F}(k)$

in the north-south direction. $D(k)$ is positive if warm air is more likely to be found in high pressure than in low. Positive $F(k)$ means that warm air occurs more frequently to the west of high pressure than to the east. Positive $D(k)$ implies more energy in the upper layer than in the lower, and positive $F(k)$ implies a northward eddy heat flux. In S78,

$$F(\mathbf{k})=U_{2n}(k)=T_{2n}(k)=D_{2n}(k)=0,$$

by the assumption of horizontal isotropy, and

$$D(\mathbf{k})=0,$$

by the imposed vertical statistical symmetry.

3. QUALITATIVE THEORY

A remarkably simple deduction based on the quadratic invariants of the motion will yield the direction of wavenumber energy transfer in stationary, homogeneous, two-layer turbulence. The deduction, which was given in S78, owes its simplicity to a choice of vertical basis which divides the total energy in horizontal wavenumber $\mathbf{k}$ into barotropic and total baroclinic components. The same theory applies to the present system. The quadratic integral invariants of the motion are the total mechanical energy, and the potential enstrophies,

$$\langle \zeta_i^2 \rangle, \quad i=1,2,$$

of each layer. It is convenient to replace the latter two by their sum and difference, which are of course also invariant. Then in the notation† of the previous section the three invariants are (proportional to):

$$\begin{aligned} I_1 &= \sum_{\mathbf{k}} U(\mathbf{k}) + E(\mathbf{k}), \\ I_2 &= \sum_{\mathbf{k}} k^2 U(\mathbf{k}) + (k^2 + k_R^2) E(\mathbf{k}), \\ I_3 &= \sum_{\mathbf{k}} (k^2 + k_R^2) D(\mathbf{k}). \end{aligned} \tag{3.1}$$

Let $\mathbf{k}$, $\mathbf{p}$, $\mathbf{q}$ be any three horizontal wavenumbers that sum vectorially to zero,

$$\mathbf{k}+\mathbf{p}+\mathbf{q}=0. \tag{3.2}$$

The energy I_1, sum enstrophy I_2, and difference enstrophy I_3 are conserved triad-wise by the nonlinear terms in the equations of motion. That is, "barotropic" triads $(\psi_{\mathbf{k}}, \psi_{\mathbf{p}}, \psi_{\mathbf{q}})$ and "baroclinic" triads $(\psi_{\mathbf{k}}, \tau_{\mathbf{p}}, \tau_{\mathbf{q}})$ respectively obey the detailed conservation laws

$$\dot{U}(\mathbf{k}) + \dot{U}(\mathbf{p}) + \dot{U}(\mathbf{q}) = 0, \quad k^2 \dot{U}(\mathbf{k}) + p^2 \dot{U}(\mathbf{p}) + q^2 \dot{U}(\mathbf{q}) = 0, \tag{3.3}$$

and

$$\dot{U}(\mathbf{k}) + \dot{E}(\mathbf{p}) + \dot{E}(\mathbf{q}) = 0, \quad k^2 \dot{U}(\mathbf{k}) + (p^2 + k_R^2)\dot{E}(\mathbf{p}) + (q^2 + k_R^2)\dot{E}(\mathbf{q}) = 0, \tag{3.4}$$

where the tendencies are those resulting from interaction with other

†This statement is true even if averaging is omitted from (3.1) because the invariants are conserved in every realization.

members in the triad.† The conservation of

$$(k^2+k_R^2)D(\mathbf{k})+(p^2+k_R^2)D(\mathbf{p})+(q^2+k_R^2)D(\mathbf{q}), \tag{3.5}$$

which places a restriction on energy transfer between layers, is actually a condition on the four *distinct* triads $(\psi_\mathbf{k},\psi_\mathbf{p},\psi_\mathbf{q})$, $(\psi_\mathbf{k},\tau_\mathbf{p},\tau_\mathbf{q})$, $(\tau_\mathbf{k},\psi_\mathbf{p},\tau_\mathbf{q})$ and $(\tau_\mathbf{k},\tau_\mathbf{p},\psi_\mathbf{q})$.

Important characteristics of the energy transfer follow directly from (3.3) and (3.4). From these two equations, one sees that the rules governing triad interactions are the same as in ordinary two-dimensional turbulence except for the interactions obeying (3.4) on scales larger than the deformation radius $(k,p,q<k_R)$. Energy transfer in the latter is a *pairwise* exchange between the two baroclinic components only; can be *nonlocal* $(p\ll q<k_R)$ in wavenumber; and can move energy efficiently toward *higher* wavenumber. There is negligible energy exchange with $U(\mathbf{k})$, except as $k\to k_R$. One can show further that, in a two-layer system in which the only energy source (e.g. solar heating) is at some low wavenumber $k_0<k_R$; and $k_D>k_R$ represents the horizontal scale at which the motion ceases to be quasi-geostrophic; the equilibrium wavenumber energy transfer must be as indicated by the solid arrows in Figure 1. The dashed arrows in the same figure indicate the direction of sum potential enstrophy flow. The argument that leads to Figure 1 leans heavily on the selection rule (3.2) and therefore applies strictly to homogeneous flow. However, it generalizes easily to flow on a spherical surface by the analogous selection rules of surface harmonics. For details, refer to S78.

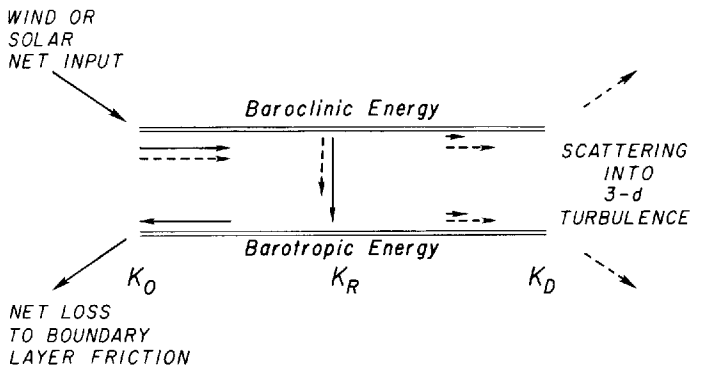

FIGURE 1 Energy (solid arrows) and sum potential enstrophy (dashed arrows) flow in wavenumber space. For an explanation, see the text.

†Note therefore that $\dot{U}(\mathbf{k})$ has, in general, a different value in (3.3) than it does in (3.4).

In the viewpoint adopted here and in S78, baroclinic instability is an extremely nonlocal interaction governed by (3.4) with $p=0$ and $k=q$. Elimination of $\dot{E}(p)$ between (3.4a) and (3.4b) gives

$$(k_R^2-k^2)\dot{U}(\mathbf{k})=k^2\dot{E}(\mathbf{k}), \tag{3.6}$$

which incidentally agrees with (2.13, 2.14). Now if $U(\mathbf{k})$ and $E(\mathbf{k})$ are infinitesimal at some initial time, then neither $\dot{U}(\mathbf{k})$ nor $\dot{E}(\mathbf{k})$ can become appreciably negative. But $\dot{U}(\mathbf{k})$, $\dot{E}(\mathbf{k})>0$ violates (3.6) unless $k<k_R$. Thus the detailed conservation laws provide an "explanation" for the stability of waves smaller than the deformation radius. If friction is present at the lower boundary, then some $k>k_R$ can be unstable even though $\dot{U}(\mathbf{k})>0$ implies $\dot{E}(\mathbf{k})<0$ by (3.6). Analysis shows that the instability occurs because friction *increases* baroclinic energy fast enough to offset the loss of baroclinic energy from interaction with the mean flow.

The non-localness of baroclinic instability suggests that it might be very susceptible to distortion by other motions with horizontal length scales between those of the mean flow and the unstable wave. For instance, local solid rotation of the whole unstable wave configuration would reduce k_x in (2.14), turn the eddy heat flux away from north, and shut off the instability. The evident source of intermediate scale energy is the leftward transfer of barotropic energy on $k<k_R$.

Imagine an initially supercritical mean shear which has been built up by solar heating. To fix ideas, let the periodic flow be infinitesimal, so that linear theory describes its initial evolution. Now obviously the exponential growth of unstable waves cannot occur indefinitely, and statistical equilibrium will somehow be reached. There are apparently at least three distinct mechanisms which can stop the exponential growth and equilibrate the flow.

First, since the energy gain of the amplifying wave represents energy lost from the mean flow, the mean shear will decrease. The rate at which solar heating replenishes the mean flow actually depends in a complicated way on the flow itself, but it must certainly be finite, and mean flow adjustment is therefore sufficient by itself to arrest the growing waves.

Second, the growing waves may eventually become large enough so that the nonlinear terms in (2.8, 2.9) are important. Then nonlinear interactions can transfer energy from the most unstable wavenumbers to stable (or less unstable) wavenumbers where dissipation occurs. The flow equilibrates when the energy input from the mean flow to the unstable waves just equals the loss by interaction with other wavenumbers.

Third, the nonlinear interactions between growing waves can reduce the correlation between northward flow (ψ_x) and warm air (τ) required by

(2.12) to maintain instability. The flow equilibrates when the correlation between $\psi_{\mathbf{k}}$ and $\tau_{\mathbf{k}}$ in every $\mathbf{k}$ is reduced to the point where the average production of turbulent energy just equals average dissipation. No actual transfer of energy between different scales is required.

The following simple stochastic model transparently exhibits an equilibration mechanism similar to the one proposed in the preceding paragraph. The model equations are:

$$\dot{\psi} + V\tau + \lambda\psi = w_1(t) - \eta\psi, \quad \dot{\tau} + V\psi + \lambda\tau = w_2(t) - \eta\tau. \tag{3.7}$$

In (3.7) V, λ and η are constants and the $w_i(t)$ are Gaussian white noise processes with covariances

$$\langle w_i(t) w_j(t') \rangle = 2D\delta_{ij}\delta(t-t'). \tag{3.8}$$

Equations (3.7) are (real) analogs for the equations for $\dot{\psi}_{\mathbf{k}}$ and $\dot{\tau}_{\mathbf{k}}$ obtained by Fourier transform of (2.8, 2.9). The right sides of (3.7) model nonlinear interactions with all other Fourier modes as a white noise forcing and stochastic damping. "Linear stability analysis" of (3.7) sets the right sides to zero and discovers instability,

$$\psi, \tau \propto \exp[\pm(V-\lambda)t], \tag{3.9}$$

if $V > \lambda$. The instability is characterized by a correlation coefficient between ψ and τ of minus unity. The Fokker–Planck equation governing the probability density $f(\psi, \tau, t)$ provides the complete statistical description of the fully "nonlinear" model. It is

$$\frac{\partial f}{\partial t} = \frac{\partial}{\partial \psi}[(V\tau + \mu\psi)f] + \frac{\partial}{\partial \tau}[(V\psi + \mu\tau)f] + D\left[\frac{\partial^2 f}{\partial \psi^2} + \frac{\partial^2 f}{\partial \tau^2}\right], \tag{3.10}$$

where

$$\mu \equiv \lambda + \eta.$$

One finds equilibrium solutions with "energy"

$$\langle \psi^2 \rangle + \langle \tau^2 \rangle = 2D/\mu(1 - V^2/\mu^2), \tag{3.11}$$

and correlation coefficient,

$$\rho \equiv \langle \psi\tau \rangle \langle \psi^2 \rangle^{-1/2} \langle \tau^2 \rangle^{-1/2} = -V/\mu, \tag{3.12}$$

provided

$$\mu > V. \tag{3.13}$$

Note that (3.13) includes shears which are unstable according to "linear" theory. Of particular interest is the case

$$\eta \equiv (V^2 - \lambda^2)/\lambda, \tag{3.14}$$

in which the turbulence contributes *no* average energy to ψ, τ. Equilibration then occurs solely because the correlation between ψ and τ is reduced by the white noise scrambling. If $\mu < V$, then the scrambling is too weak and the system eventually blows up. A more faithful analog (e.g. the turbulence model introduced below) would have built in that the strength of nonlinearity increases, on average, with the energy in ψ, τ.

Certainly each of the three "mechanisms" discussed above plays a role in atmospheric dynamics. I suggest, however, that the second and particularly the third have not received the attention they deserve. It is conceivable, of course, that nonlinear interactions reinforce rather than inhibit instability. However, other ideas suggest that the effects of strong nonlinearity on baroclinic instability are destructive on average, and can be very efficient.

Suppose that forcing and damping are omitted from the two-layer equations so that the flow conserves energy and enstrophy exactly. Statistical equilibrium cannot then be reached. In such flow the enstrophy spreads toward higher wavenumbers indefinitely. However, if the equations of motion are artificially truncated (as always necessary in practice) by removal of all triad interactions that involve at least one wavenumber $\mathbf{k}$ with $k > k_c$, say, for some cutoff wavenumber k_c, then the truncated equations approach a special, "thermal" equilibrium which may be predicted by classical methods. The underlying theory has been discussed elsewhere (Lee, 1952; Salmon *et al.*, 1976; Kriachnan and Montgomery, 1979).

Thermal equilibrium is the final state towards which nonlinear interactions acting alone would drive the flow. The two-layer thermal equilibrium states (with periodic geometry) are all horizontally isotropic, and nearly barotropic on scales larger than the internal deformation radius. The latter fact suggests that an unstable baroclinic current does *not* stop losing energy when its vertical shear drops below the critical value predicted by linear theory, provided that the growing waves have reached sufficient amplitude for the flow to become turbulent. Numerical experiments, particularly those of Rhines (1976), confirm that unreplenished large-scale baroclinicity virtually disappears in a turn-over time. However, in the strongly forced numerical experiments described below, the equilibrium mean flow is always supercritical for some $\mathbf{k}$. This implies

that baroclinic instability in these wavenumbers is arrested primarily by processes other than the depletion of the mean flow. Interestingly, if the mean shear is held constant at an arbitrary supercritical value, then similar experiments show that the periodic flow still equilibrates, despite the lack of any bound on energy.

Consider next the possibility of energy transfer out of the band of unstable wavenumbers (mechanism two). If $\beta=0$, then (neglecting friction) all wavenumbers $\mathbf{k}$ with $k<k_R$ are unstable. The invariants of the motion trap most of the energy within this band so that energy transfer to the stable wavenumbers greater than k_R is ineffective. (However, there is no constraint against transfer from modes with larger to smaller k_x that occurs if the elongated eddies associated with instability become isotropic without a change in scale.)

In thermal equilibrium $F(\mathbf{k})=0$, and it is therefore plausible that nonlinear interactions reduce the correlation between warm and north-flowing air (mechanism three). Since $F(\mathbf{k})$ is absent from (3.1), no fundamental conservation principle directly inhibits this reduction. Unlike energy, which disappears at one wavenumber only by appearing at another, the correlation quantity $F(\mathbf{k})$ can simply vanish.

If $\beta\neq 0$ there is a stable band at low k. However, no fundamental conservation principle like (3.6) prevents direct energy transfer from the mean flow into these wavenumbers in the finite-amplitude case. The numerical experiments reported in the next section show that the effects of β on two layer flow are actually quite subtle.

4. SIMULATION EXPERIMENTS

This section reports three numerical experiments in which (2.1–2.3) were first stepped to equilibrium and then integrated for a time (twenty weeks) judged long enough to yield accurate low-order statistics. The experiments, which are summarized in Table II, differed only in their values of β and λ. In all four experiments, V was computed from

$$\frac{d}{dt}E_M=-P+S, \tag{4.1}$$

where

$$E_M=(1.4\times 10^5\,\text{joule sec}^{-2}\,\text{m}^{-4})V^2 \tag{4.2}$$

is the available energy (per unit area) in the mean flow, P is the rate of turbulent energy production given by (2.12), and

$$S=3.00\,\text{watt m}^{-2} \tag{4.3}$$

TABLE II

Summary of simulation and closure experiments

Experiment	A	B	C	AA	CC
Simulation (S) or closure (C)	S	S	S	C	C
Duration (weeks)	20	20	20	—	—
k_R	8	8	8	8	8
$\beta(10^{-13}\,\mathrm{cm^{-1}\,sec^{-1}})$	0.0	1.0	1.0	0.0	1.0
λ^{-1} (days)	1.85	1.85	3.7	1.85	3.7
$\langle V\rangle$ ($\mathrm{m\,sec^{-1}}$)	2.36	4.88	4.68	2.41	4.53
Energy ($10^5\,\mathrm{j\,m^{-2}}$):					
Barotropic	9.57	12.92	16.41	9.24	15.40
Baroclinic kinetic	3.01	3.36	2.99	2.84	3.15
Available potential	13.40	10.33	10.02	12.17	9.39
Total baroclinic	16.41	13.69	13.01	15.01	12.54
Total mechanical	25.98	26.61	29.42	24.25	27.94
Ratio of kinetic energy in the bottom 500 mb to that in the top	0.228	0.183	0.286	0.227	0.266

is a prescribed constant rate of solar input to the mean energy. The coefficient in (4.2) is such that a representative equilibrium shear of $V=4\,\mathrm{m\,sec^{-1}}$ gives $E_M=22\times10^5\,\mathrm{joule\,m^{-2}}$. In equilibrium, the size of the coefficient serves principally to control the variance of V. The prescribed energy input (4.3) corresponds to strong winter circulation.

The equations of motion were solved spectrally by expanding the dependent variables in truncated Fourier series,

$$(\psi,\tau)=\sum_{|\mathbf{k}|<16}(\psi_{\mathbf{k}},\tau_{\mathbf{k}})e^{i\mathbf{k}\cdot\mathbf{x}}, \tag{4.4}$$

and then solving the resulting set of coupled ordinary differential equations using Orszag's (1971) staggered-grid algorithm. The finite truncation in $\mathbf{k}$ requires that enstrophy be removed from the vicinity of $k=16$ by an eddy viscosity. The eddy viscosity is similar to that used in S78:

$$(\dot{\zeta}_i)_{\mathbf{k}}=\text{other terms}-(\alpha_{\mathbf{k}})_i(\zeta_i)_{\mathbf{k}}, \tag{4.5}$$

$$(\alpha_{\mathbf{k}})_1=\begin{cases}\nu_0 k_c^2\dfrac{(k^2-k_R^2)^2}{(k_c^2-k_R^2)^2}, & k>k_R\\ 0, & k<k_R\end{cases}$$

$$(\alpha_{\mathbf{k}})_2=\gamma(\alpha_{\mathbf{k}})_1,\quad \gamma=0.2,$$

$$k_c=15,$$

$$\nu_0=5.4\times10^{-3}\,\text{days}.$$

The numerical constants that appear in (4.5) were chosen simply to give the wavenumber spectra a smooth appearance near k_c.

Figure 2 shows the wavenumber spectra for experiments A, B, and C. The kinetic energy spectra (Figures 2a-b) all have peaks at wavenumbers 3 or 4. I believe that these peaks may agree with atmospheric observations. Remember that the model mean flow has a delta function spectrum at $k=0$ which does not appear in Figure 2. The analog of k on the spherical earth is the degree n of surface harmonic function Y_{nm}. In the real atmosphere the "mean flow", that is those scales directly forced by solar

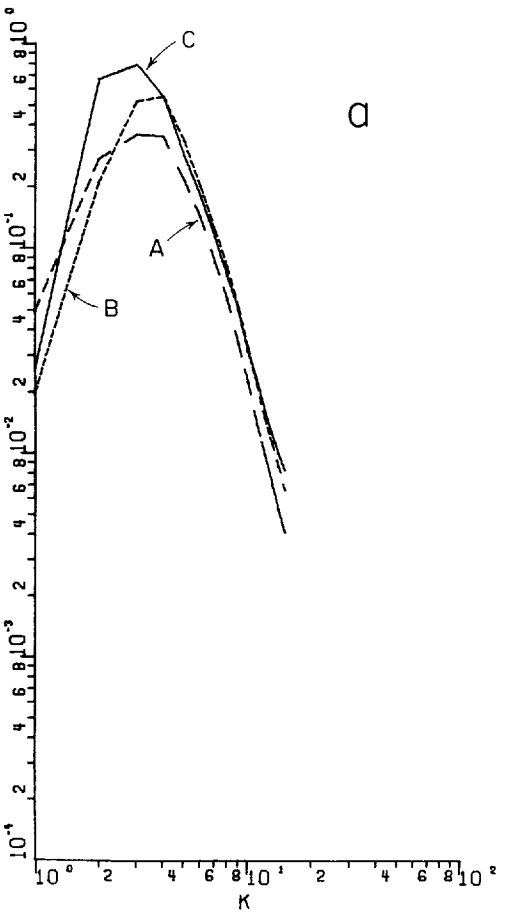

FIGURE 2 The energy spectra (a) $U(k)$, (b) $\bar{T}(k)$, (c) $\bar{E}(k)$ and (d) $\bar{F}(k)$; and (e) the ratio of lower to upper layer kinetic energy in wavenumber k; for experiments A, B, and C. The vertical scale is arbitrary. The maxima in (e) near $k=16$ are an artifact of the choice of γ.

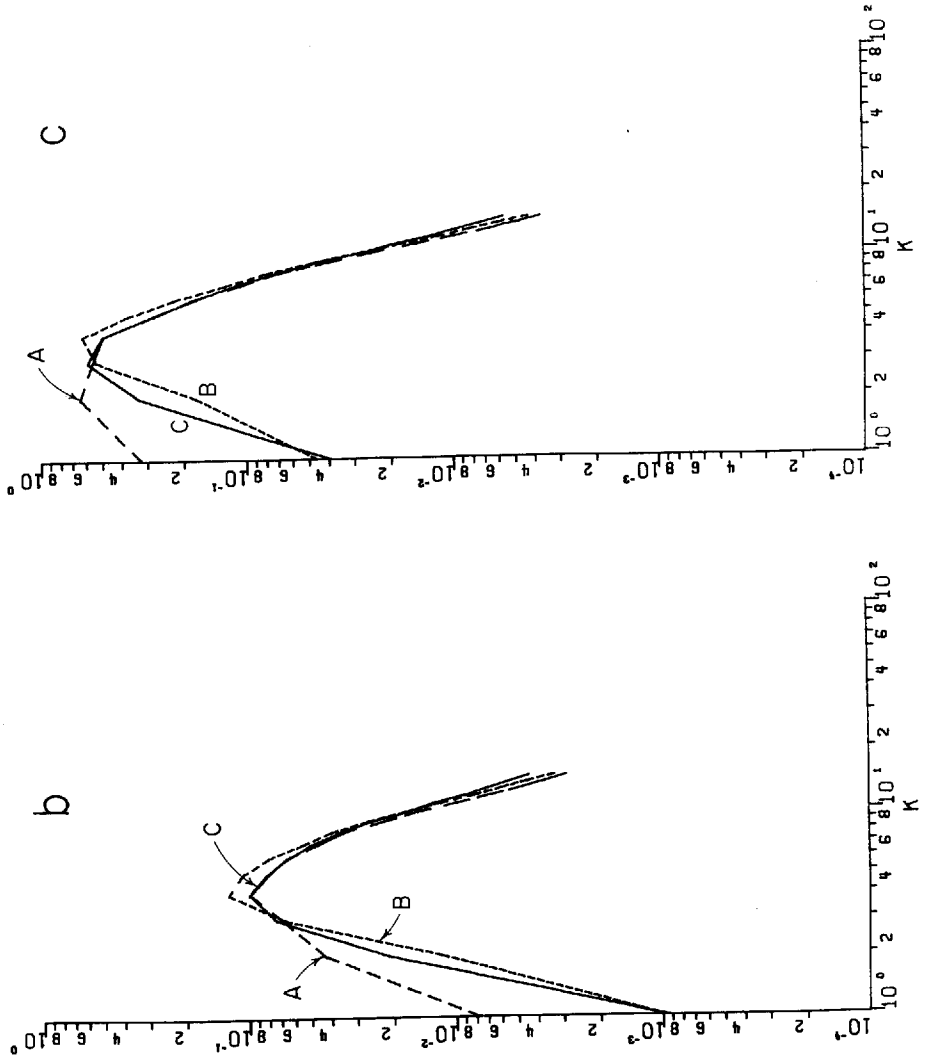

FIGURE 2(b–c).

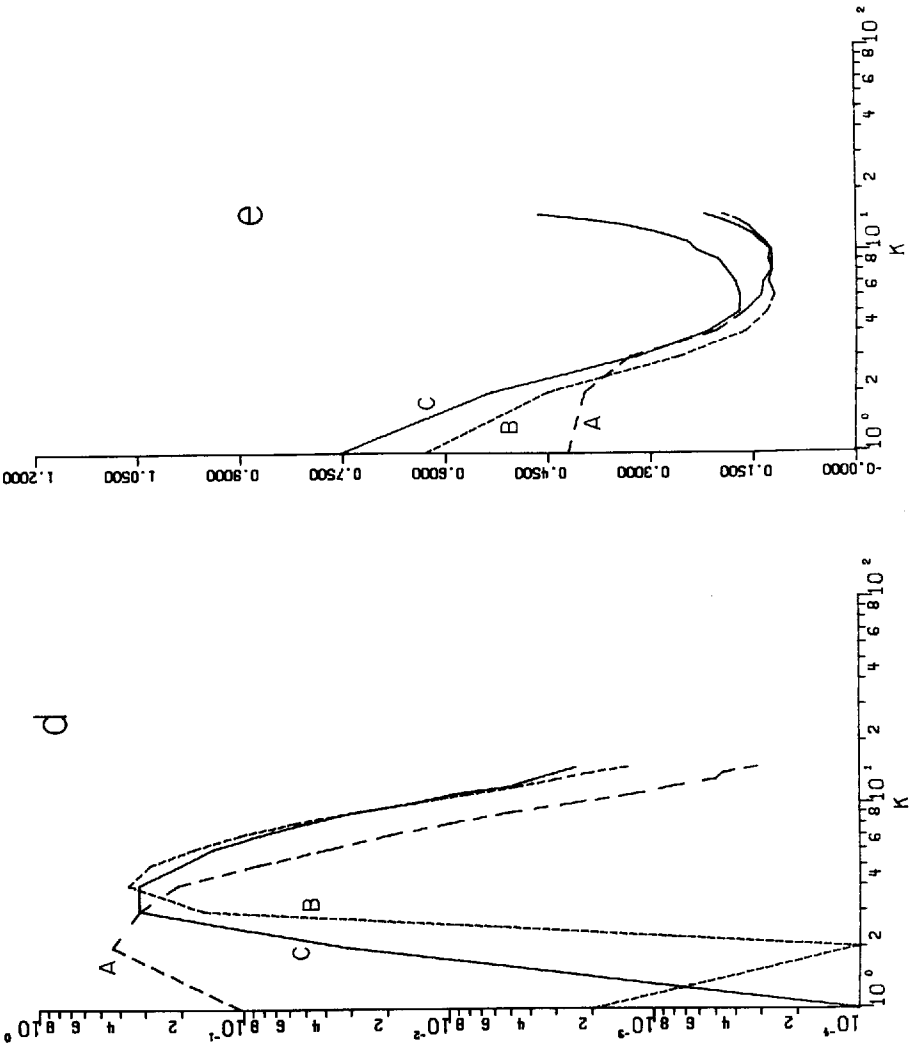

FIGURE 2(d–e).

heating, resides primarily in $n=1$, and the present experiments would suggest a spectral gap in kinetic energy between $n=1$ and $n=3,4$. Figure 3 shows the kinetic energy spectrum based on n calculated by Chen and Wiin-Nielsen (1978) from 14 months of northern hemisphere data. This spectrum supports a gap between $n=1$ and 4.

The most striking differences in Figure 2 are between experiments with and without beta. The experiment with $\beta=0$ has lower barotropic energy and a higher baroclinic energy, which resides primarily in wavenumbers 1 and 2 (Figure 2c). The higher baroclinic energy is obviously related to a higher production $F(k)$ on these wavenumbers (Figure 2d). The simple

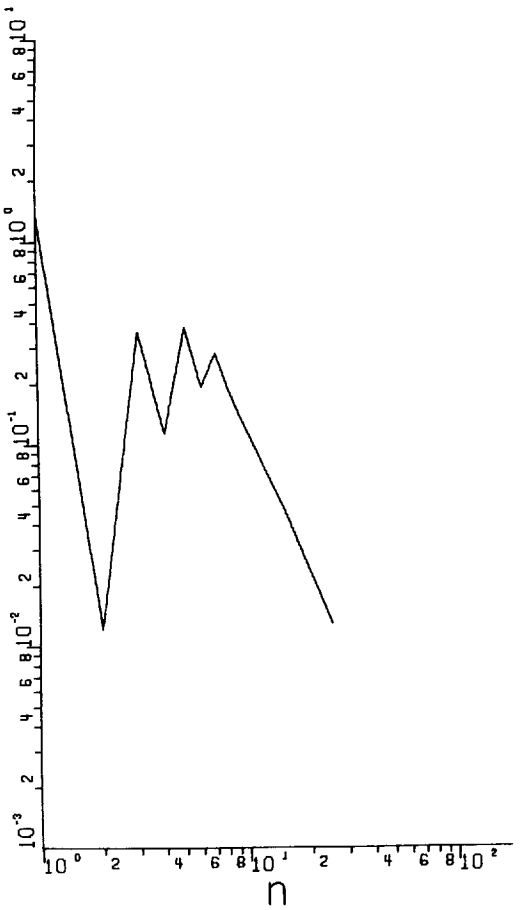

FIGURE 3 The vertically integrated kinetic energy as a function of n, the degree of surface harmonic. After Chen and Wiin-Nielsen (1978).

ideas of the previous section can explain these differences. From (3.6), which governs baroclinic instability whether or not beta is zero, it follows that the ratio of production by instability of baroclinic energy to the production of barotropic energy decreases with increasing k on $k<k_R$. This ratio is unity for

$$k=2^{-1/2}k_R=5.6 \tag{4.6}$$

Thus experiments B and C with non-zero beta and dominant transfer of mean flow energy into $k=3,4$ have a larger equilibrium ratio of barotropic to baroclinic energy than does experiment A with no beta and significant production in $k=1,2$. Whether beta is zero or not, the direction of baroclinic energy transfer is toward still larger k on $k<k_R$, and the anticipated "final state" with nonlinearity acting alone would be nearly barotropic flow irrespective of beta. (Note that beta does not appear in the quadratic integral invariants and therefore does not influence thermal equilibrium in this geometry.) However, apparently because of the shorter initial "cascade step", much less energy actually reaches barotropic mode in the case $\beta=0$ before it is wiped out by friction. Curiously then, although beta stabilizes the flow, it also moves the system more quickly toward the endpoint of Figure 1 by forcing the rightward transfer of energy on $k<k_R$ to be more nonlocal in k than if $\beta=0$. Note the contrast with leftward energy transfer in purely two-dimensional flow, in which beta always slows wavenumber energy transfer (Rhines, 1975; Holloway and Hendershott, 1977).

The evident source for very large scale ($k=1,2$) baroclinic energy in experiment B and C is back-transfer of energy in baroclinic triads. The baroclinic energy on these scales is in fact so small that $J(\tau,\nabla^2\tau)$ scales out of (2.8). Thus the dominant nonlinear tendencies in (2.8, 2.9) on $k<3$ with $\beta\neq 0$ are

$$\nabla^2\psi_t+J(\psi,\nabla^2\psi)=0, \tag{4.7}$$

and

$$\tau_t+J(\psi,\tau)=0, \tag{4.8}$$

which are the equations for advection of a passive scalar in two-dimensional flow. The thermal equilibrium state corresponding to (4.7, 4.8) has equipartition of $\langle|\tau_{\mathbf{k}}|^2\rangle$ in every $\mathbf{k}$. By (2.21) and (2.24) this corresponds to a baroclinic kinetic energy spectrum $\bar{T}(k)$ proportional to k^{+3}. Interestingly, $\bar{T}(k)$ in experiments B and C is indeed very close to k^{+3} on $k=1$ to 3. The back-transfer of baroclinic energy has therefore apparently saturated low wavenumbers.

Leftward transfer of barotropic energy is slowed by the beta effect and attenuated by ground friction which destroys barotropic more efficiently than baroclinic energy on large scales. However, the shape of $\bar{U}(k)$ is remarkably invariant to changes in β and λ. The explanation is that Ekman friction removes energy from wavenumber k at a rate which is independent of k, whereas any reasonable estimate for the time required to move energy from some k to, say, $k/2$ gives a time that increases with decreasing k.

In all three experiments, the peak in kinetic energy occurs slightly below the wavenumber of fastest growth predicted by linear stability analysis on the time-averaged shear $\langle V \rangle$ (Table III). However, the average shear is highly supercritical on $0 < k < k_R$ when $\beta = 0$ and on $4 < k < k_R$ when $\beta \neq 0$. Note from Table III and Figure 4 that the shear fluctuates by less than 10% of its average value in all three experiments so that the above statements are true also for the instantaneous shear. The stability analysis summarized in Table III includes the ground friction.

TABLE III

Mean flow supercriticality

Experiment	A	B	C
$\langle V \rangle \pm$standard deviation	2.36 ± 0.15	4.88 ± 0.14	4.68 ± 0.15 m sec^{-1}
Minimum critical V	2.1×10^{-3}	1.78	1.75 m sec^{-1}
Wavenumber of minimum critical V	6.3	8.4	8.3
Wavenumber of fastest growth at experimental average $\langle V \rangle$	4.0	5.6	5.7
Critical V at the latter wavenumber	2.2×10^{-2}	2.51	2.43 m sec^{-1}
Wavenumber of maximum $F(k)$	2	4	3–4
Wavenumber where $\langle V \rangle$ would be critical	—	3.7	3.8

In all three experiments, motion at wavenumbers higher than the peak in kinetic energy ($k \geqq 3$) is nearly isotropic (Figure 5). In experiment A, positive anisotropy associated with instability appears only on $k = 1, 2$. This gives the largest scale motions an advantage over smaller scales in tapping energy from the mean flow. Remember that $U_2(k)$, $T_2(k) > 0$ correspond to elongation of streamfunction fields in the north-south direction. In the two experiments with $\beta \neq 0$, negative anisotropy appears in barotropic mode at the lowest wavenumbers because leftward transfer of barotropic energy favors zonal flow (Rhines, 1975; Holloway, 1976). The negative anisotropy in baroclinic mode in experiments B and C must come from straining by the zonal barotropic flow through (4.8).

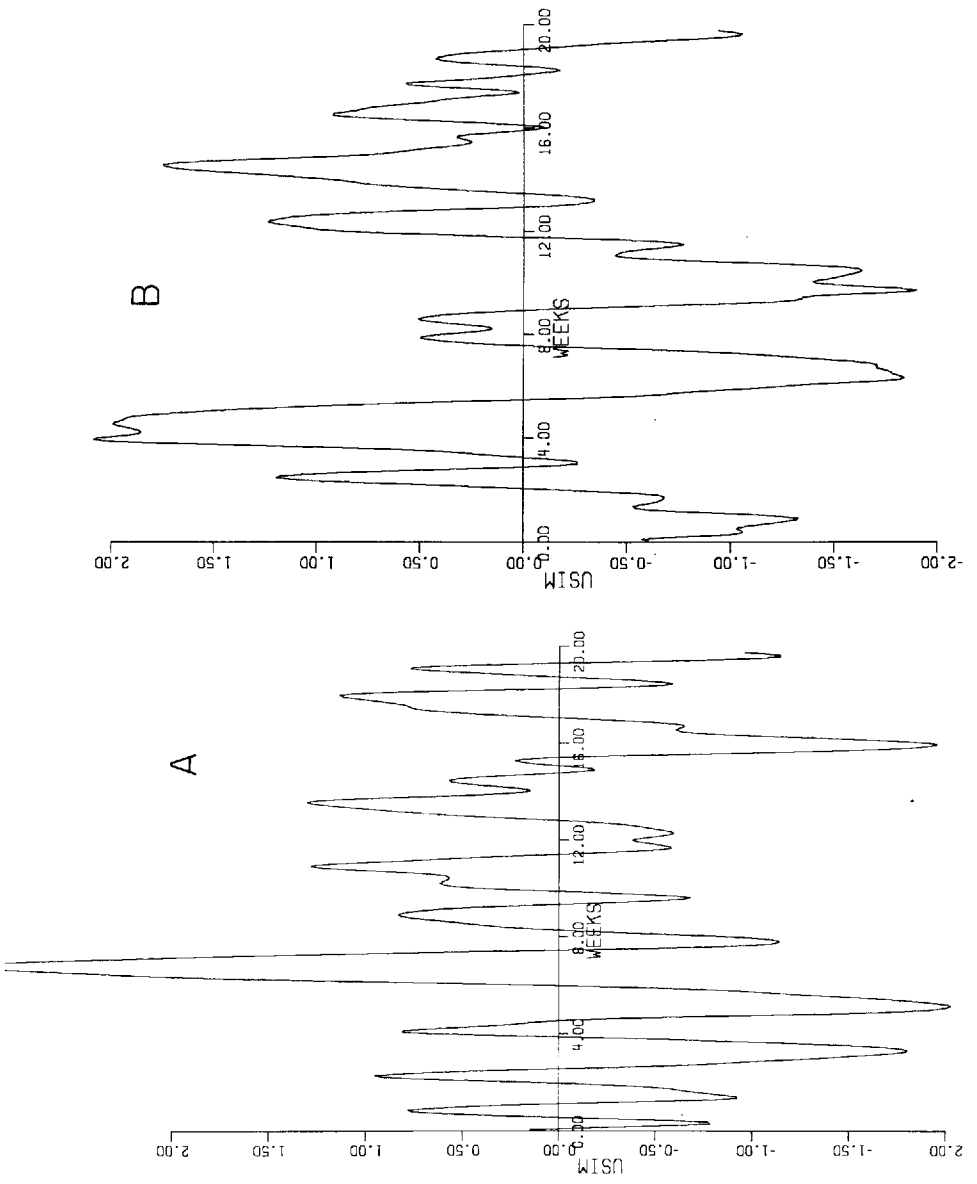

FIGURE 4. The mean shear $V(t)$ in experiments A, B, and C. Vertical scale in units of one standard deviation (about 0.15 m sec^{-1}).

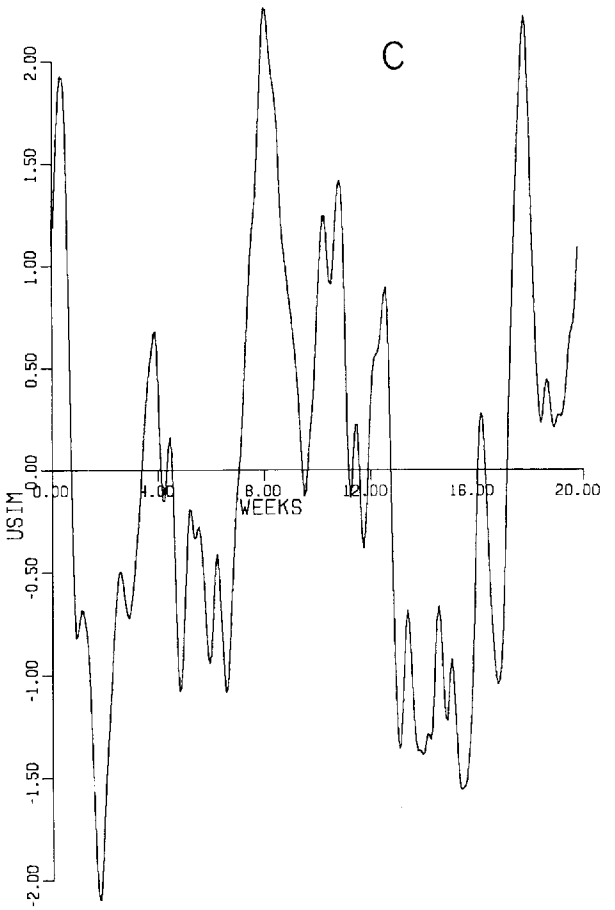

The biggest discrepency between the fully nonlinear experiments and linear theory is the high supercriticality of the experimental mean flow with respect to the higher unstable wavenumbers and the fact that these wavenumbers contribute little to the total production of energy from the mean flow. $U_2 = T_2 = 0$ in these wavenumbers has the effect of lowering the linear growth rate (2.14), but does not change the exponential nature of the instability. The primary task of the closure analysis begun in the next section will be to isolate as far as possible the mechanism of nonlinear equilibration.

5. THE CLOSURE

Turbulence closure models of the direct interaction (DIA) family model the true flow as a Gaussian random field and then make corrections to

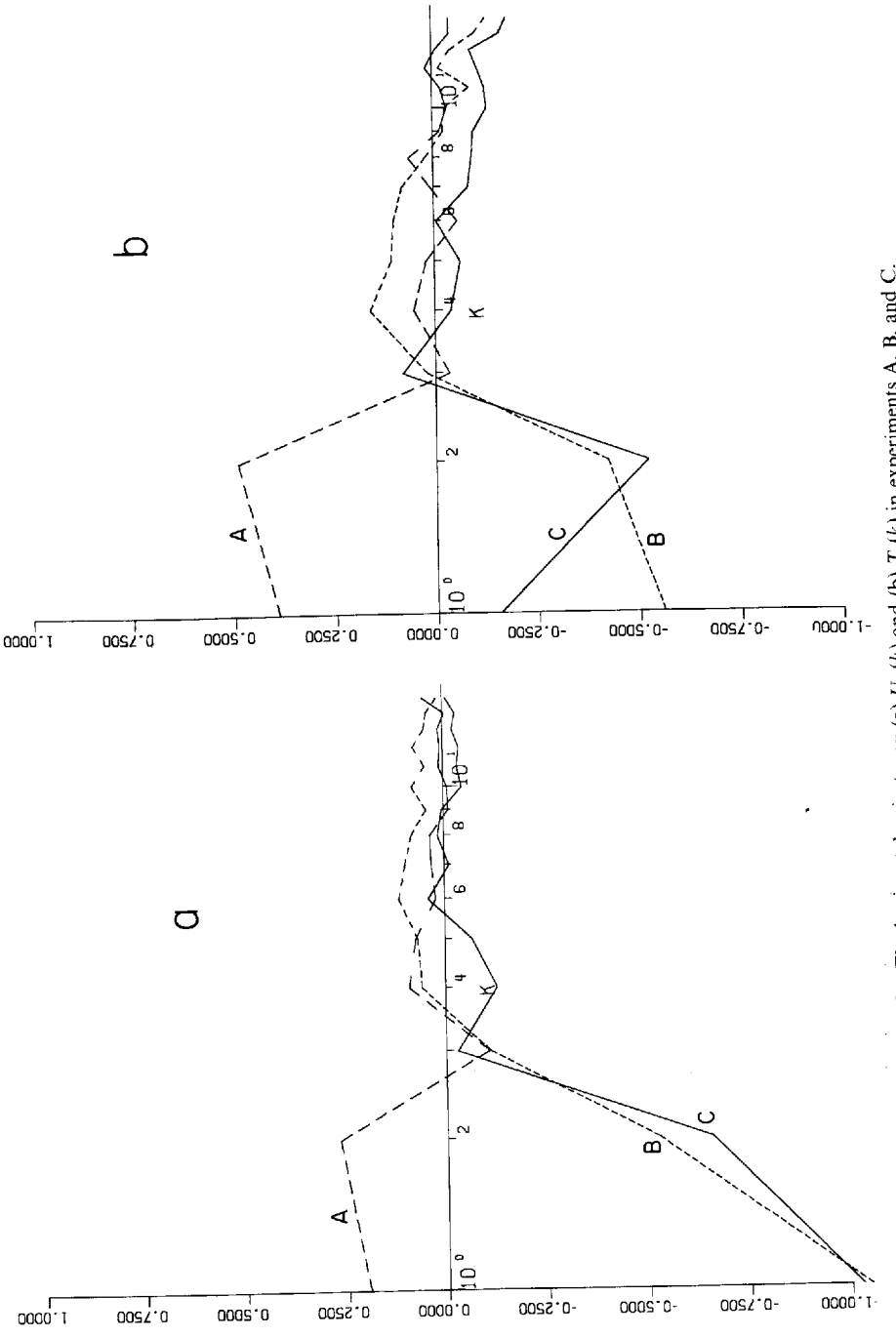

FIGURE 5. The horizontal anisotropy (a) $U_2(k)$ and (b) $T_2(k)$ in experiments A, B, and C.

preserve quadratic invariants and relaxation to thermal equilibrium. Alternatively, these closures can be "derived" by a variety of perturbation-like procedures, none of which pretends to mathematical rigor. Two of the most physically appealing procedures are Kraichnan's (1959) original derivation of the DIA and Orszag's (1970) eddy-damped Markovian (EDM) model. In this paper I use a slight extension of the Markovian random coupling (MRC) model of Frisch *et al.* (1974). It is much simpler than either DIA or EDM in the present case. The extension consists of replacing the constant time factor which appears in MRC by the triad relaxation time factors prescribed by the test field model (Kraichnan, 1971a). This section provides a technical description of the closure. Readers who are uninterested in these details should skip ahead to Section 6.

Let

$$\dot{y}_i = L_{ij} y_j + A_{ijk} y_j y_k \tag{5.1}$$

represent an arbitrary dynamical equation with quadratic nonlinearity. In (5.1) L_{ij} and A_{ijk} are constant factors, the subscripts identify modes, and the summation convention is in effect. The MRC provides a closed set of equations for the evolution of second moments $\langle y_i y_j \rangle$. The closure equation is exact not for (5.1), but for the related set of model equations

$$\dot{y}_i^a = L_{ij} y_j^a + N^{-1} W_{abc}(t) A_{ijk} y_j^b y_k^c, \tag{5.2}$$

in the limit $N \to \infty$. In (5.2) the superscript summations extend from 1 to N and the $W_{abc}(t)$ are independent white noise processes with identical covariance factors. The summation over b and c in (5.2) can be viewed as an arbitrarily imposed random coupling between N realizations of the flow. Note the curious analogy between the dynamical model (5.2) and a common assumption of spectral estimation theory that different modes of a single realization may be treated as independent estimates. For the details of the derivation of the moment equation from (5.2) refer to Frisch *et al.* (1974).

In practice, the MRC moment equations are most easily obtained by the following formal procedure which I illustrate by application to (2.8, 2.9). Write the Fourier transform of (2.8, 2.9) in the compressed form

$$\dot{\psi}_{\mathbf{k}}^i = C_{\mathbf{k}}^{il} \psi_{\mathbf{k}}^l + \sum_{\mathbf{p}+\mathbf{q}=\mathbf{k}} A_{\mathbf{kpq}}^{imn} \psi_{\mathbf{p}}^m \psi_{\mathbf{q}}^n, \tag{5.3}$$

where $\psi_{\mathbf{k}}^i$ is defined by (2.17),

$$A_{\mathbf{kpq}}^{imn} \equiv \tfrac{1}{2}(p_x q_y - q_x p_y)(\bar{q}^2 - \bar{p}^2)\Delta_{imn}/\bar{k}^2, \tag{5.4}$$

and

$$\bar{k}^2 \equiv \begin{cases} k^2, & \text{if } i=0, \\ k^2+k_R^2, & \text{if } i=1, \end{cases} \tag{5.5}$$

and similarly for $\bar{p}$ and $\bar{q}$. The summation convention applies to superscripts only. In (5.3) $C^{il}_{\mathbf{k}}$ are constant coefficients that depend on V, β, and λ. Here V will be treated as a constant. In (5.4) $\Delta_{imn}=1$ if $i=m=n=0$ or if exactly two of i, m, n are unity. Otherwise $\Delta_{imn}=0$.

The formal procedure consists of the following steps:

i) Omitting temporarily the linear terms, expand the solution to (5.3) in a Taylor series in time about $t=0$, and truncate the series after order t^2;

$$\psi^i_{\mathbf{k}}(t)=\psi^i_{\mathbf{k}}(0)+t\dot{\psi}^i_{\mathbf{k}}(0)+\tfrac{1}{2}t^2\ddot{\psi}^i_{\mathbf{k}}(0), \tag{5.6}$$

ii) Regard the intial conditions as Gaussian with zero mean.

iii) Form the Taylor series expansion of $R^{ij}_{\mathbf{k}}(t)$ about $t=0$ by multiplying (5.6) and averaging. Use the factorization property of Gaussian variables.

iv) Differentiate the result with respect to time, replace the factor t by a constant (say t_0), and restore all arguments to t.

v) Re-insert the linear terms as they would occur in the exact second moment equations.

The extension of MRC referred to above consists of the following final step:

vi) Replace t_0 by $\theta_{\mathbf{kpq}}$, defined below.

The result of steps (i–vi) is:

$$\dot{R}^{ij}_{\mathbf{k}}=C^{il}_{\mathbf{k}}R^{lj}_{\mathbf{k}}+C^{jl}_{-\mathbf{k}}R^{il}_{\mathbf{k}}+\sum_{\mathbf{p}+\mathbf{q}=\mathbf{k}}4\theta_{\mathbf{kpq}}\{A^{imn}_{\mathbf{kpq}}A^{jvv}_{\mathbf{kpq}}R^{mw}_{\mathbf{p}}R^{nv}_{\mathbf{q}}$$
$$+A^{imn}_{\mathbf{kpq}}A^{mwv}_{\mathbf{pk}-\mathbf{q}}R^{nv}_{\mathbf{q}}R^{wj}_{\mathbf{k}}+A^{jmn}_{\mathbf{kpq}}A^{mwv}_{\mathbf{pk}-\mathbf{q}}R^{vn}_{\mathbf{q}}R^{iw}_{\mathbf{k}}\}. \tag{5.7}$$

In the full EDM, the triad relaxation time $\theta_{\mathbf{kpq}}$ carries six modal superscripts and there would be seven (instead of four) superscript summations in (5.7). Note that many terms in (5.7) are zero. The nonlinear part of (5.7) conserves all quadratic invariants and satisfies the realizability conditions

$$U(\mathbf{k}), T(\mathbf{k})\geqq 0, \tag{5.8}$$

$$U(\mathbf{k})+T(\mathbf{k})\geqq 2D(\mathbf{k}), \tag{5.9}$$

and

$$U(\mathbf{k})\cdot T(\mathbf{k})\geqq D(\mathbf{k})^2+F(\mathbf{k})^2. \tag{5.10}$$

This follows directly from the fact that (5.8–5.10) hold for arbitrary truncations of the Taylor series.

In this paper I set

$$\theta_{\mathbf{kpq}}=\frac{\eta_{\mathbf{k}}+\eta_{\mathbf{p}}+\eta_{\mathbf{q}}}{(\eta_{\mathbf{k}}+\eta_{\mathbf{p}}+\eta_{\mathbf{q}})^2+(\omega_{\mathbf{p}}+\omega_{\mathbf{q}}+\omega_{-\mathbf{k}})^2} \tag{5.11}$$

which has the form proposed by Holloway and Hendershott (1977). In (5.11),

$$\omega_{\mathbf{k}}=-\beta k_x/k^2 \tag{5.12}$$

is the dispersion relation for barotropic Rossby waves and $\eta_{\mathbf{k}}$ is the decorrelation rate prescribed by the test field model (Kraichnan, 1971a) for two-dimensional flow with the same velocity spectrum as the 500 mb horizontal velocity field. (The order one constant that appears in the test field model is set equal to unity.) The above prescription for $\theta_{\mathbf{kpq}}$ in two-layer flow is obviously quite arbitrary. However, experience has shown that equilibrium solutions to closure equations like (5.7) are rather insensitive to the specific choice of relaxation factor.

The next section compares equilibrium solutions of (5.7) and (4.1) with the spectra obtained by averaging the direct simulations.

6. CLOSURE EXPERIMENTS

This section reports two closure experiments, AA and CC, which were performed with the same parameter settings as simulation experiments A and C (the two most different experiments). Figures 6 to 9 compare steady equilibrium solutions to (5.7) and (4.1) with the spectra obtained by time-averaging the simulations. Table II compares gross energy levels. The overall agreement between the simulations and closure is very good. This agreement is by itself significant because it means that the closure model, despite its arbitrariness and lack of fundamental justification, successfully mimics the behavior of the nonlinear terms in the exact equations of motion at least to the extent of producing accurate second moment statistics. Unlike (2.8) and (2.9), (5.7) is amenable to analytic simplification. An example will be given below.

I next examine the equilibrium balance of terms in the closure equation for $F(\mathbf{k})$. To aid the subsequent analysis it is convenient, at the same time, to write the sums in (5.7) as integrals. The equation is

$$\dot{F}(\mathbf{k})=0=\text{linear terms}+\text{nonlinear terms}. \tag{6.1}$$

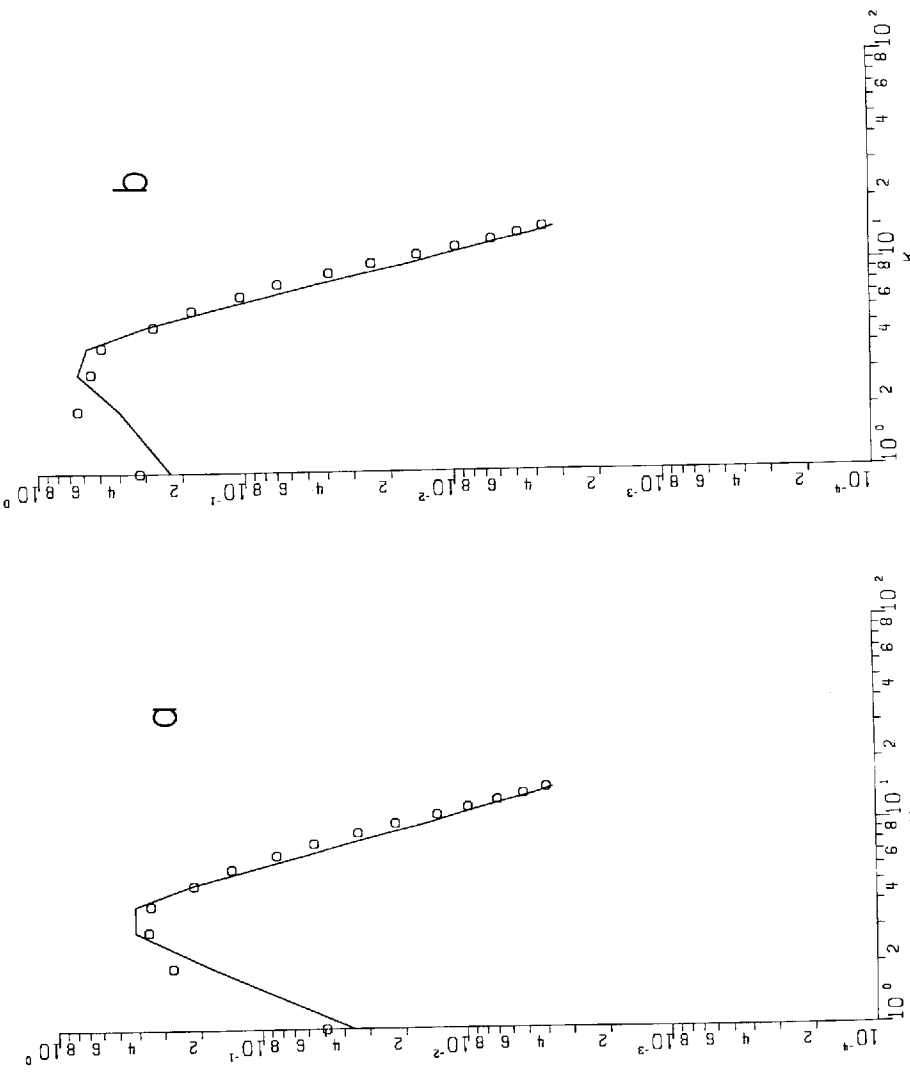

FIGURE 6. The energy spectra (a) $\bar{U}(k)$ and (b) $\bar{E}(k)$ and the production (c) $F(k)$ for simulation A (circles and closure AA (solid line). Arbitrary vertical scale.

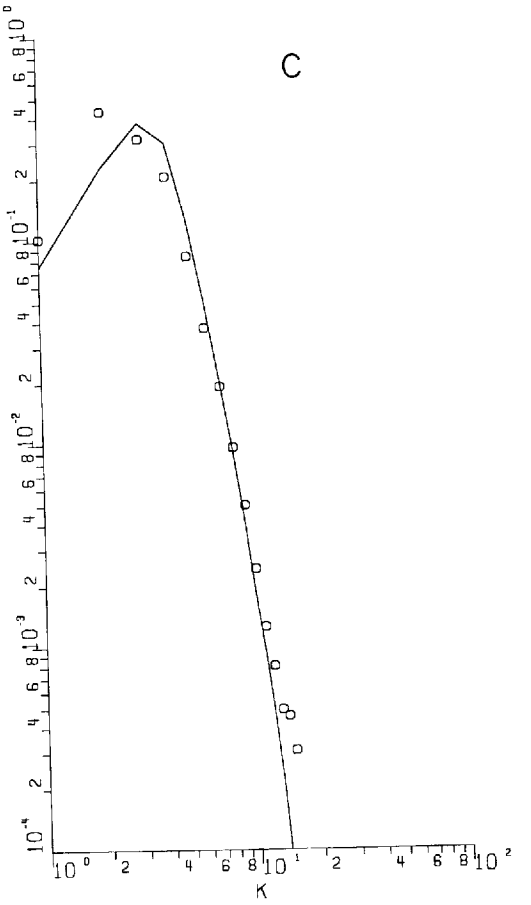

where

$$\text{linear terms} = -[k_x \beta k_R^2 / k^2 (k^2 + k_R^2)] D(\mathbf{k}) + k_x V T(\mathbf{k}) + k_x V (k_R^2 - k^2)(k_R^2 + k^2)^{-1} U(\mathbf{k}) + \text{friction}, \tag{6.2}$$

and

$$\text{nonlinear terms} = \int d\mathbf{p} \int d\mathbf{q}\, \theta(\mathbf{k}, \mathbf{p}, \mathbf{q}) \sin^2 K\, \delta(\mathbf{p} + \mathbf{q} - \mathbf{k}) U(\mathbf{q}) \times \{2(q^2 - p^2)(q^2 - p^2 - k_R^2)(k^2 + k_R^2)^{-1} F(\mathbf{p}) - (q^2 - p^2)(q^2 - k^2) k^{-2} F(\mathbf{k}) - p^2 (q^2 - p^2 - k_R^2)(q^2 - k^2 - k_R^2)(k^2 + k_R^2)^{-1} (p^2 + k_R^2)^{-1} F(\mathbf{k})\} + \text{other nonlinear terms from (5.7)}. \tag{6.3}$$

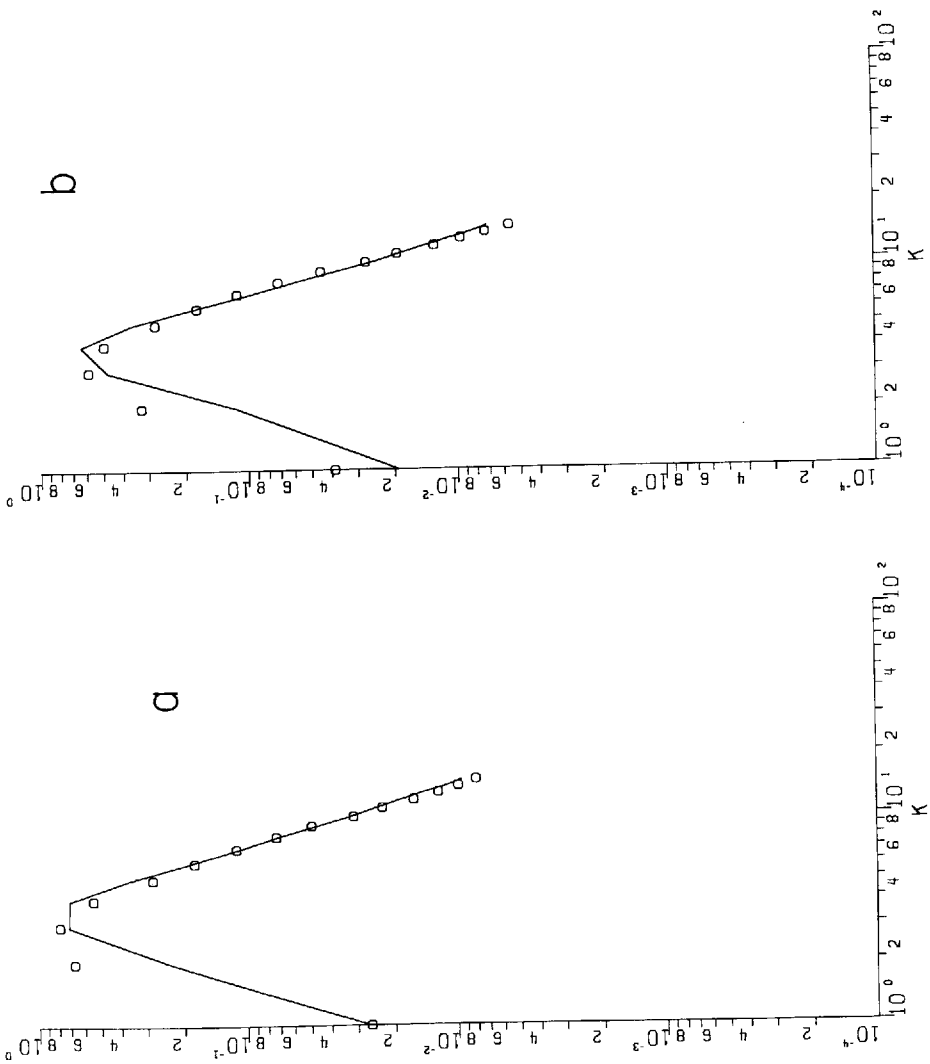

FIGURE 7. The same as figure 6 for experiment C and closure CC.

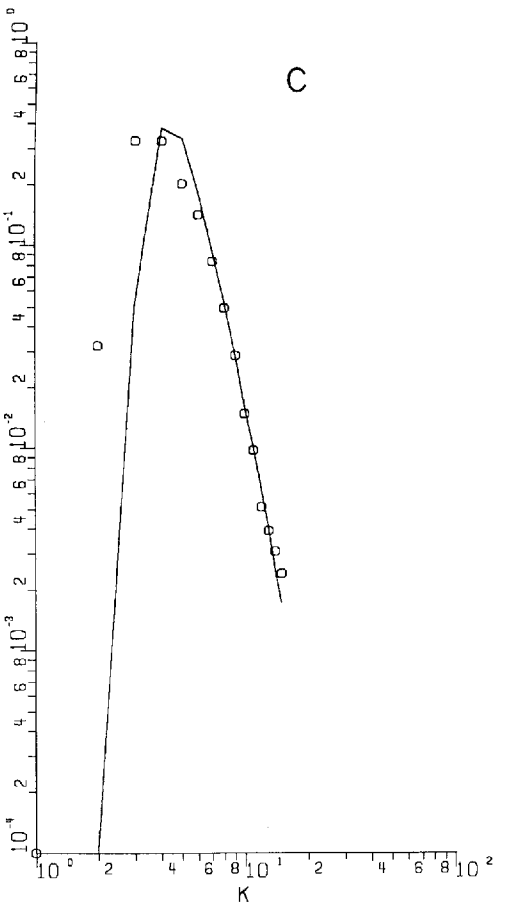

In (6.3) K is the angle opposite the side of length k in the triangle with sides of lengths k, p, q. The other symbols have been previously defined.

It can be shown from the closure experiments that the three nonlinear terms written out explicitly in (6.3) comprise nearly all of the nonlinear contribution to $\dot{F}(\mathbf{k})$ on the linearly unstable wavenumber range. Figure 10 shows the total nonlinear contribution to $\dot{F}(k_x, 0)$ in experiment CC and the contribution to the same from the three terms in (6.3) and from the sum of all remaining nonlinear terms. (The results for experiment AA are qualitatively similar and will not be shown.) Figure 11 graphs the three nonlinear terms individually for the same experiment. In Figures 10 and 11 solid lines denote positive values and dashed lines denote negative values. Note from Figure 11 that the third term in (6.3) dominates the sum at the

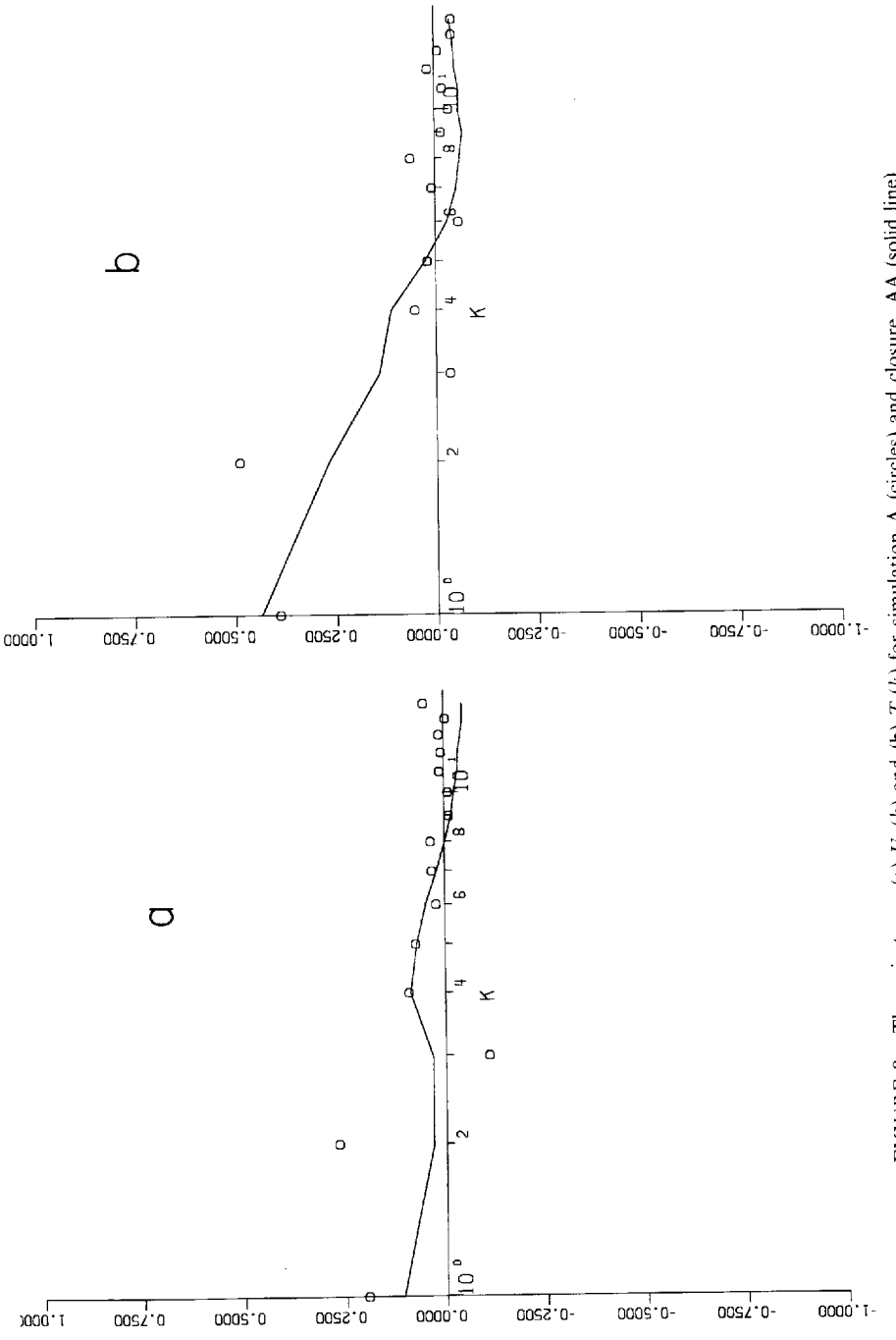

FIGURE 8. The anisotropy (a) $U_2(k)$ and (b) $T_2(k)$ for simulation A (circles) and closure AA (solid line).

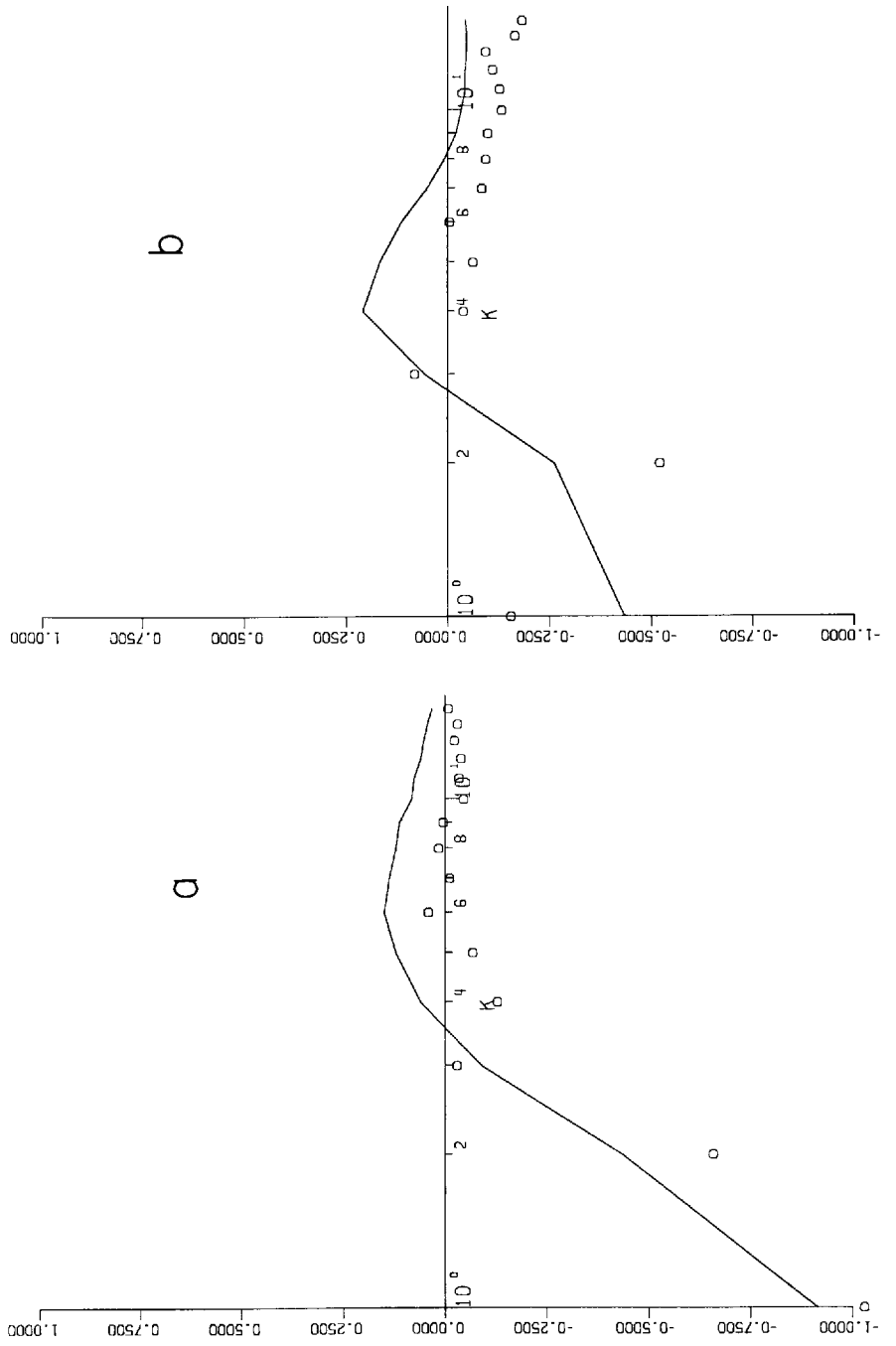

FIGURE 9. The same as figure 8 for simulation C and closure CC.

wavenumbers of maximum production $F(\mathbf{k})$, but that at the higher unstable wavenumbers there is near cancellation between the three terms.

In (6.3) assume that $k^2 \ll k_R^2$ and that the dominant contributions to the integrals come from $p^2, q^2 \ll k_R^2$. Assume further that

$$U(\mathbf{k}) = U(k), \tag{6.4}$$

and

$$F(\mathbf{k}) = F(k)\cos\theta. \tag{6.5}$$

which amounts to a truncation of (2.22) and (2.23). This truncation is

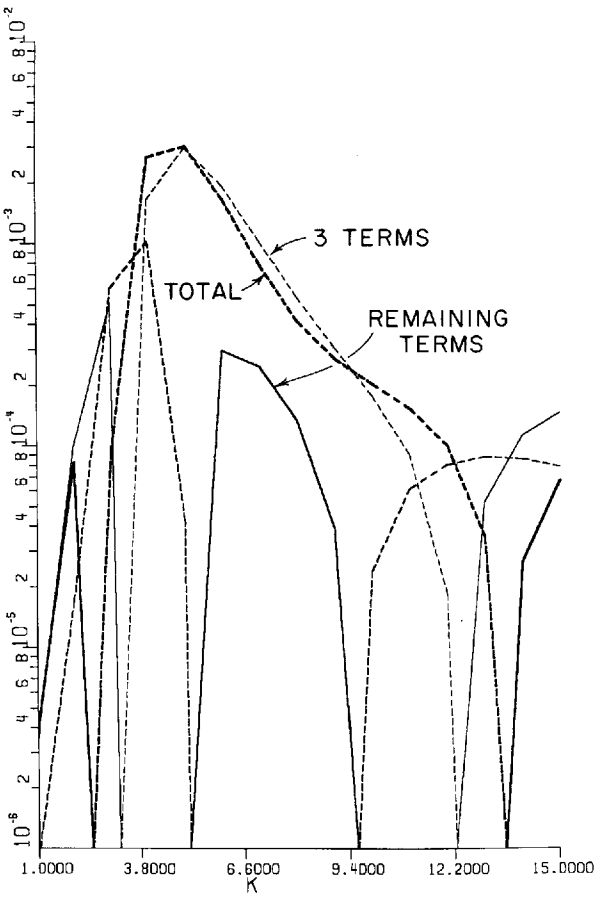

FIGURE 10. The total nonlinear contribution to the change in $F(k)$ and the contribution to same from the three terms written out explicitly in (6.3) and from the remaining nonlinear terms.

justified by both the simulations and closure, except perhaps at $k=1$. Substitute (6.4, 6.5) into (6.3) and change the integration variables from $\mathbf{p}$, $\mathbf{q}$ to p, θ_p, q, θ_q where

$$\mathbf{p}=p(\cos\theta_p, \sin\theta_p) \quad \text{and} \quad \mathbf{q}=q(\cos\theta_q, \sin\theta_q).$$

If, for convenience, $\theta(\mathbf{k},\mathbf{p},\mathbf{q})$ is assumed to depend on the wavenumber magnitudes only, then the integration over θ_p and θ_q can be performed. One finds that

$$\int d\mathbf{p}\int d\mathbf{q}\,\delta(\mathbf{p}+\mathbf{q}-\mathbf{k})=2\overset{\Delta}{\iint} dp\,dq\sin^{-1}K, \tag{6.6}$$

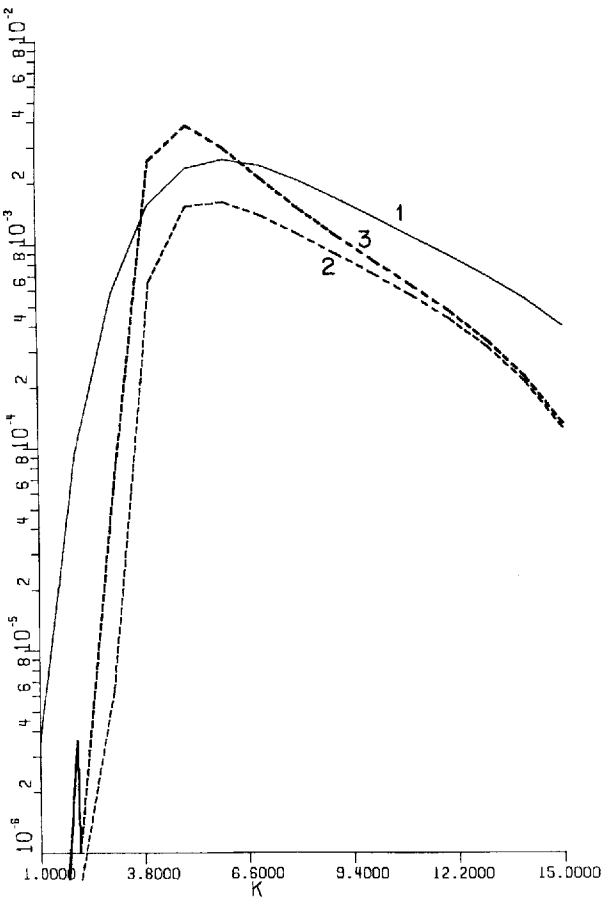

FIGURE 11. The contribution to the change in $F(k)$ from each of the three terms written out explicitly in (6.3).

and

$$\frac{1}{2\pi}\int_0^{2\pi} d\theta \int d\mathbf{p} \int d\mathbf{q}\, \delta(\mathbf{p}+\mathbf{q}-\mathbf{k}) \cos\theta \cos\theta_p = 2\iint_{\Delta} dp\, dq \cos Q \sin^{-1} K, \quad (6.7)$$

where Δ is the region of the positive $p-q$ quadrant for which a triangle with sides k, p, q can exist. Then (6.3) becomes

$$\dot{F}(k) = \iint_{\Delta} dp\, dq\, \theta(k,p,q) \sin K\ U(q)$$
$$\{4(p^2-q^2)\cos Q\ F(p) - 2(q^2-p^2)(q^2-k^2)k^{-2}F(k) - 2p^2F(k)\} + \ldots \quad (6.8)$$

The assumption that k^2, p^2, $q^2 \ll k_R^2$ assures that (6.8) has the same form as if the governing nonlinear dynamics had been (4.7) and (4.8), the advection of passive scalar τ by a two-dimensional velocity field with stream function ψ and spectrum $U(q)$. It is then easy to verify that the third term is the only term of (6.8) which survives if (4.7) is dropped and the barotropic field treated as a random *time-invariant* flow. This means that the third term in (6.8), which balances linear instability near $k=4$, results solely from the advection of the temperature field by barotropic flow and that changes in the barotropic flow itself, which contribute to the first and second terms in (6.8), have secondary importance at $k=4, 5$. The third term in (6.8) is in fact proportional to the "damping" term in the corresponding equation for the spectrum of a passively advected scalar in isotropic two-dimensional flow. Thus the nonlinear attenuation of the correlation quantity $F(k)$ near the peak of $F(k)$ must result primarily from scattering of baroclinic energy from the peak wavenumbers to other (chiefly higher) wavenumbers by the barotropic advecting field.

Figure 12 shows a four-day sequence from experiment C during which the total production declined from a maximum of 5.31 watts m^{-2} at record 207 to a minimum of 1.83 watts m^{-2} at record 214 and then rose again to 3.59 watts m^{-2} by record 217. A number of such sequences have been examined. The beginning of the sequence corresponds to the maximum of production near week 13 in Figure 13. Note that this size variation is typical of the whole record. The lower pictures in Figure 12 shows the total 500 mb streamfunction, $\psi - 1.6Vy$, in solid lines and the 500 mb temperature $\tau - Vy$ in dotted lines. Darker contours correspond to higher values. The upper pictures contour the product $\psi_x \tau$ of the northward velocity and the perturbation temperature. The spatial integral of the upper pictures is proportional to the total production. At the beginning of the sequence the largest contribution from the production comes from the strong feature in the upper center of the picture. The positive correlation

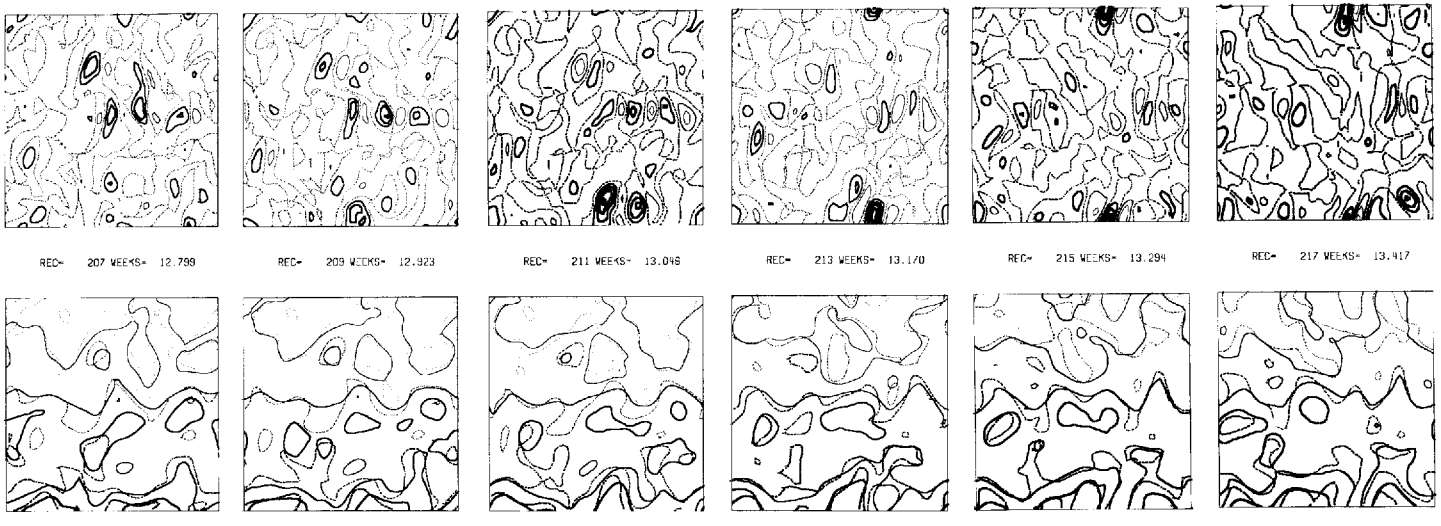

FIGURE 12. (a), (b) and (c). Lower pictures: the 500 mb total streamfunction (solid contours) and temperature (dotted contours) in a 4-day sequence from Experiment C. Upper pictures: contours of the product of northward velocity and perturbation temperature at the corresponding times. In the upper picture the dotted contour is the zero contour. In all pictures, darker lines denote higher values of contoured quantity. For a complete explanation, refer to the text.

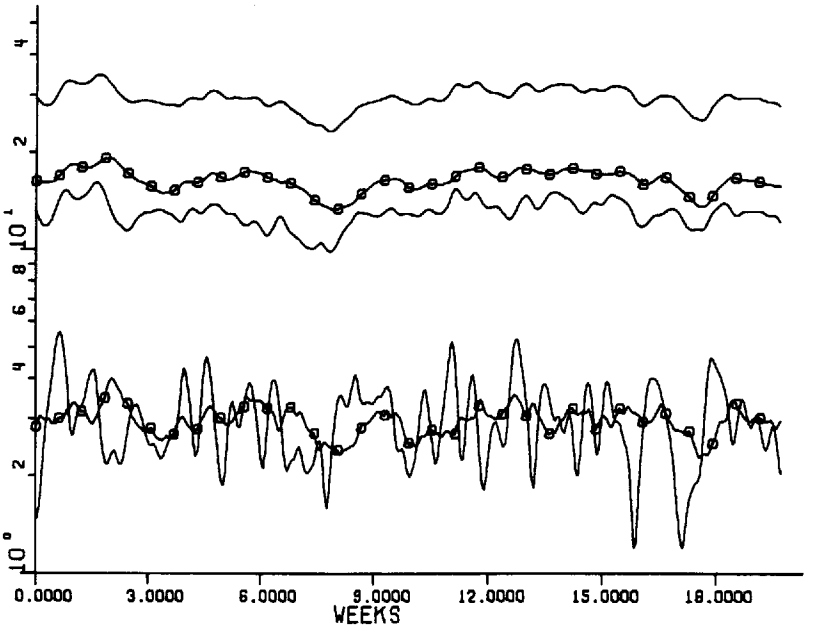

FIGURE 13. The total energy (upper solid curve), total barotropic energy (upper curve with symbols), total baroclinic energy (middle solid curve), production (lower solid curve), and dissipation (lower curve with symbols) in experiment C. Units of 10^5 joule m^{-2}, and watt m^{-2}.

between temperature and northward flow is easy to see. Note that both fields have closed contours. In the following pictures the warm center to the west of the closed high moves clockwise around the high and production decreases. The streamfunction perturbation weakens and moves westward. When sites of strong production again develop in the final picture of the sequence, they do so in another region of the flow. More than anything perhaps, Figure 12 illustrates the difficulty of separating out "processes" from individual realizations of complicated flow patterns.

Figure 11 shows that all three terms in (6.8) are important for the higher unstable wavenumbers ($k \geqq 6$) and that the second and third terms tend to cancel the first. The physical interpretation of these terms is now more difficult, but it is of interest because the low production rate $F(\mathbf{k})$ in these highly supercritical wavenumbers is perhaps the biggest discrepancy between the linear theory and the fully nonlinear experiments.

I begin by deriving an approximation to (6.8) assuming that the dominant contribution to the integrals comes from $q < k'$ where k'/k is small. In (6.8) restrict the integration region to $q < \varepsilon k$, change the

integration variables to

$$p' = (p-k)/\varepsilon k,$$

and (6.9)

$$q' = q/\varepsilon k,$$

and expand the entire right side of (6.8) in powers of ε, performing all quadratures. The arithmetic is tedious but straightforward. At the first order, terms two and three in (6.8) are equal and precisely cancel term one, in encouraging agreement with Figure 11. At the first non-vanishing order the approximation gives

$$\dot{F}(k) \sim \theta(k,k,0)\tfrac{1}{4}\pi\Omega\left\{\frac{1}{K}\frac{\partial}{\partial k}\left(k^3\frac{\partial F}{\partial k}\right) - 3F(k)\right\}, \tag{6.10}$$

wnere

$$\Omega = \int_0^{\varepsilon k} dq\, U(q) q^3 \tag{6.11}$$

and possible k-dependence of $\theta(k,k,0)$ has been neglected. In the next section I will obtain (6.10) without the use of closure (but with a strong assumption about the velocity field). The goal of this exercise is additional physical insight.

7. THE MECHANISM OF NONLINEAR EQUILIBRATION

Before proceeding, it will help to review related other work. Equation (6.10) without the term $3F(k)$ is identical to the equation for the spectrum of passive scalar ϕ advected by a two-dimensional white-noise isotropic straining field ψ in which motions on scale k^{-1} make a negligible contribution to the straining (Kriachnan, 1974). The equations are

$$\partial\phi/\partial t + J(\psi,\phi) = 0, \tag{7.1}$$

$$S(k) = \langle \phi_{\mathbf{k}} \phi_{-\mathbf{k}} \rangle, \tag{7.2}$$

$$U(k) = k^2 \langle \psi_{\mathbf{k}} \psi_{-\mathbf{k}} \rangle, \tag{7.3}$$

and

$$\dot{S}(k) = \theta(k,k,0)\tfrac{1}{4}\pi\Omega\frac{1}{k}\frac{\partial}{\partial k}\left(k^3\frac{\partial S}{\partial k}\right), \tag{7.4}$$

where Ω is given by (6.11). The steady solutions to (7.4) are the viscous-convection range, $kS(k) \sim k^{-1}$, of Batchelor (1959) and thermal equilibrium, $S(k) = \text{constant}$. Note that (7.4) conserves scalar variance, $\int kS(k)\,dk$. According to closure, Eq. (7.4) with $S(k)$ replaced by $k^2U(k)$ also governs the energy spectrum in the enstrophy inertial range of two-dimensional turbulence (Kraichnan, 1971).

The diffusion-like form of (7.4) can be related to random stretchings of ϕ by the large scale straining motion (Kraichnan, 1974). The following analysis will show that the $3F(k)$ term in (6.10) results from rotations of the advected structures about a local vertical axis, and that rotation is typically three or more times as important as stretching because both strain and vorticity contribute to local rotations.

Let the scalar field ϕ be a local sinusoid of wavevector $\mathbf{k}$ in the vicinity of $x = y = 0$. Then the change in $\mathbf{k}$ following a fluid particle is given by

$$dk_j/dt = -k_i A_{ij}, \tag{7.5}$$

where

$$A_{ij} = \partial u_i/\partial x_j. \tag{7.6}$$

The summation convention is in effect. Equation (7.5) is in a sense the reciprocal of a more familiar equation for the rate of change of an infinitesimal line element $\mathbf{r}$,

$$dr_i/dt = A_{ij} r_j. \tag{7.7}$$

Note that

$$\frac{d}{dt}(\mathbf{r} \cdot \mathbf{k}) = 0. \tag{7.8}$$

Regard the advecting field $\psi(x, y, t)$ as given. Equation (7.5) is still difficult to solve because the right side must be continually re-evaluated along the trajectory of the particle. However, exact results are obtainable if ψ is white noise in time.

Let the spatial correlation scale of ψ be large compared to k^{-1}. Then

$$\psi = \tfrac{1}{2}\zeta_0(x^2 + y^2) + \tfrac{1}{2}S_0(x^2 - y^2) + \sigma_0 xy, \tag{7.9}$$

locally in the vicinity of $x = y = 0$. Here $\zeta(x, y, t)$ is the vorticity and $S(x, y, t)$ and $\sigma(x, y, t)$ the strain rates, and

$$\zeta_0 = \zeta(0, 0, t), \quad S_0 = S(0, 0, t), \quad \sigma_0 = \sigma(0, 0, t). \tag{7.10}$$

If ψ is isotropic then ζ, S, and σ are independent and

$$\langle\zeta^2\rangle = 2\langle S^2\rangle = 2\langle\sigma^2\rangle = \tfrac{1}{2}\pi\Omega, \tag{7.11}$$

where

$$\Omega = \int k^3 U(k)\, dk. \tag{7.12}$$

In (7.9), let ζ_0, S_0, σ_0 be independent Gaussian random variables with covariances

$$\langle\zeta_0(t)\zeta_0(t')\rangle = 2D_\zeta\delta(t-t'), \tag{7.13}$$

and

$$\langle S_0(t)S_0(t')\rangle = \langle\sigma_0(t)\sigma_0(t')\rangle = 2D_S\delta(t-t'), \tag{7.14}$$

where

$$D_\zeta = 2D_S = \pi\Omega\theta_0. \tag{7.15}$$

The constant θ_0 (units of time) may be interpreted as the "effective half-width" of the covariance functions. It will eventually identify with $\theta(k,k,0)$ above. With (7.9), (7.5) becomes

$$dk_1/dt = -S_0k_2 + \sigma_0k_1 - \zeta_0k_2,\ dk_2/dt = -S_0k_1 - \sigma_0k_2 + \zeta_0k_1. \tag{7.16}$$

The Fokker–Planck equation governing the joint probability distribution $f(k_1, k_2, t)$ of the components k_1, k_2 follows from (7.13–7.16) by standard methods. (See, for example, Soong (1973), page 182.) It is

$$\frac{\partial}{\partial t} f(k,\theta) = D_S \frac{1}{k}\frac{\partial}{\partial k}\left(k^3\frac{\partial f}{\partial k}\right) + (D_S + D_\zeta)\frac{\partial^2 f}{\partial\theta^2}, \tag{7.17}$$

where the independent variables have been changed from k_1, k_2 to k, θ defined by

$$\mathbf{k} = k(\cos\theta, \sin\theta).$$

Not surprisingly, (7.17) is a diffusion equation in both wavenumber magnitude k and direction θ. The k-operator is identical to that in (7.4) and comes solely from straining, but both straining and vorticity contribute to the diffusion in direction of $\mathbf{k}$. However, since $D_\zeta = 2D_S$ local solid roation is twice as important as the rotations that accompany straining.

Equation (7.17) governs the probability distribution of an ensemble of

passively advected wavevectors. It also governs the evolution of any averaged quantity, expressed as a function of $\mathbf{k}$ and t, which is conserved on particles. In particular, (7.17) governs scalar variance $S(k,\theta,t)$ and it is the generalization of (7.4) to anisotropic scalar distribution. In the present limit (7.17) also governs $F(\mathbf{k},t)$. This follows from the definition (2.21d) and the conservation of the vorticity and temperature wave amplitudes and their phase difference. Substitution of (6.5) into (7.17) gives

$$\frac{\partial F}{\partial t}=D_S\frac{1}{k}\frac{\partial}{\partial k}\left(k^3\frac{\partial F}{\partial k}\right)-(D_S+D_\zeta)F, \tag{7.18}$$

which agrees exactly with (6.10) if $\theta_0=\theta(k,k,0)$.

It is easy to show that both stretching and rotation typically reduce the production $\int F(k)\,dk$. Integration of (7.18) between k_1 and k_2 gives

$$dP_{12}/dt=[Q(k_2)-Q(k_1)-D_SP_{12}]-(D_S+D_\zeta)P_{12} \tag{7.19}$$

where

$$P_{12}\equiv\int_{k_1}^{k_2}F(k)\,dk \quad\text{and}\quad Q(k)\equiv k^2\frac{\partial F}{\partial k}+kF.$$

The square brackets in (7.19) enclose the contribution of the k-operator term. Obviously the Q terms represent the flux of $F(k)$ from outside the region $[k_1,k_2]$ of applicability of (7.18). Inspection of the remaining terms in (7.19), and use of (7.15), shows that rotation is asymptotically three times more efficient than stretching in reducing the production. If higher angular harmonics ($\cos n\theta$) are present in the expansion (2.21d) of $F(\mathbf{k})$ then the ratio of the rotation to the stretching terms is even greater (increasing as n^2).

Finally, if I relax the assumption that k^2, p^2, $q^2\ll k_R^2$ in (6.3), then (6.10) generalizes to

$$\dot{F}(k)\sim\theta(k,k,0)\tfrac{1}{4}\pi\Omega\left\{\frac{1}{k(k^2+k_R^2)}\frac{\partial}{\partial k}\left[k^3\frac{\partial}{\partial k}[(k^2+k_R^2)F]\right]-3F\right\}, \tag{7.20}$$

which has the same form as if the governing nonlinear dynamics had been (4.7) and (4.8) but with τ replaced by $\nabla^2\tau-k_R^2\tau$. As expected, (7.20) is equivalent to (7.17) with

$$f(k,\theta)=(k^2+k_R^2)F(k)\cos\theta. \tag{7.21}$$

The previously stated conclusions are qualitatively unchanged.

8. FINAL REMARKS

This study has addressed what seemed to me to be the most fundamental question about the general circulation whose answer lies wholly outside the realm of linear mechanics. The two-level model with uniform mean flow is probably the simplest model which might have been used. However, its deficiencies as a general circulation model are many. Here I shall mention only those which seem to me to be the most distressing.

The climatological mean jet stream—probably the most distinctive feature of the general circulation besides the westerlies themselves—has been spread out over the entire flow domain and the mean vertical shear correspondingly reduced. My use of solar mechanical energy input appropriate for January is perhaps a partial compensation, but it is not really clear, for example, whether the model statistics ought to be compared to winter hemispherical averages or annual averages over the vicinity of the jet. There is no gradient of mean westerly momentum.

The imposed periodicity enforces an infinite horizontal scale separation between the average flow and the transient waves which is particularly unrealistic for the lowest nonzero wavenumbers. That is, model wavenumber 1 "sees" a mean flow which is infinitely broader than itself whereas no such infinite separation is possible on the finite globe. I can say, however, that there is apparently nothing anomalous about the model inviscid statistical mechanics: when solar heating and friction were suddenly switched off in experiment C, the mean flow decreased steadily below the minimum critical value according to linear theory.

Gall *et al.* (1979) have considered some factors which affect the wavelength of maximum northward heat transport in the NCAR primitive equation general circulation model. Linear stability analysis on the model predicts fastest growth at a wavenumber higher than 12, but the maximum transport in his experiments occurs at wavenumbers nearer 7. Gall appeals to rapid increases in the low-level static stability to explain why "intermediate scale" waves eventually reach a greater amplitude than the "short" waves. In my study, the static stability is held constant, and shallow high-wavenumber instability cannot occur because of the simpler mean flow and dynamics. Here, the primary focus is on "intermediate" and "very long" wavelengths.

Stone (1978) finds that the real atmosphere is baroclinically stable south of the mean jet stream when the observations are analyzed with a "local" two-level model. However, my highly supercritical mean flow apparently disagrees with his findings that the observed flow north of the jet is near critical. Stone (personal communication) suspects that the increase in local static stability (decrease in k_R) that accompanies baroclinic instability may

be the most important mechanism of adjustment, and might explain the high supercriticality in the present study. The critical mean shear is in fact very sensitive to k_R ($V_{\text{crit}} = \beta/k_R^2$). However, it is not easy to decide what value of k_R (or what parameterization for change in k_R) best fits the real atmosphere to the two-level dry model. It may be that questions about criticality can only be answered within the context of a model with prescribed dynamics.

Acknowledgement

This study was supported by the National Science Foundation (grant No. ATM-7818388).

References

Batchelor, G. K. "Small-scale variations of convected quantities like temperature in turbulent fluid," *J. Fluid Mech.*, **5,** 113 (1959).

Charney, J. G. and Phillips, N. A. "Numerical integration of the quasi-geostrophic equations for barotropic and simple baroclinic flows," *Journ. Met.*, **10,** 71 (1952).

Chen, T.-C. and Wiin-Nielsen, A. "On nonlinear cascades of atmospheric energy and enstrophy in a two-dimensional spectral index," *Tellus*, **30,** 313 (1978).

Frisch, U., Lesieur, M. and Brissaud, A. "A Markovian random coupling model for turbulence," *J. Fluid Mech.*, **65,** 145 (1974).

Gall, R., Blakeslee, R. and Somerville, R. C. J. "Baroclinic instability and the selection of the zonal scale of the transient eddies of mid-latitude," *J. Atmos. Sci.*, **36,** 767 (1979).

Haltiner, G. J., *Numerical Weather Prediction.* Wiley, New York (1971).

Held, I. M. "The vertical scale of an unstable baroclinic wave and its importance for eddy heat flux parameterization," *J. Atmos. Sci.*, **35,** 572 (1978).

Holloway, G. "Statistical hydromechanics: applications in mesoscale ocean circulation," Ph.D. thesis, Univ. Cal. San Diego (1976).

Holloway, G. and Hendershott, M. C. "Stochastic closure for nonlinear Rossby waves," *J. Fluid Mech.*, **82,** 747 (1977).

Kraichnan, R. H. "The structure of isotropic turbulence at very high Reynolds numbers," *J. Fluid Mech.*, **5,** 497 (1959).

Kraichnan, R. H. "Inertial range transfer in two- and three-dimensional turbulence," *J. Fluid Mech.*, **47,** 525 (1971).

Kraichnan, R. H. "An almost-Markovian Galilean-invariant turbulence model," *J. Fluid Mech.*, **47,** 513 (1971a).

Kraichnan, R. H. "Convection of a passive scalar by a quasi-uniform random straining field," *J. Fluid Mech.*, **64,** 737 (1974).

Kraichnan, R. H. and Montgomery, D. "Two-dimensional turbulence," submitted to *Rep. Prog. Phys.*, 1979.

Lee, T. D. "On some statistical properties of hydromechanical and magneto-hydrodynamical fields," *Q. J. Appl. Math.*, **10,** 69 (1952).

Moura, A. D. and Stone, P. H. "The effects of spherical geometry on baroclinic instability," *J. Atmos. Sci.*, **33,** 602 (1976).

Orszag, S. A. "Analytical theories of turbulence," *J. Fluid Mech.*, **41,** 363 (1970).

Orszag, S. A. "Numerical simulation of incompressible flows within simple boundaries," *Stud. Appl. Math.*, **L,** 293 (1971).

Pedlosky, J. "The stability of currents in the atmosphere and ocean," *J. Atmos. Sci.*, **21,** 201 (1964).

Rossby, C. G. "Relation between variations in the intensity of the zonal circulation of the atmosphere and the displacement of the semi-permanent centers of action," *J. Mar. Res.*, **2,** 38 (1939).

Rhines, P. B. "Waves and turbulence on a beta-plane," *J. Fluid Mech.*, **69,** 417 (1975).

Rhines, P. B. "The dynamics of unsteady currents," in *The Sea*, vol. VI, John Wiley and Sons, New York (1976).

Salmon, R., Holloway, G. and Hendershott, M. C. "The equilibrium statistical mechanics of simple quasi-geostrophic models," *J. Fluid Mech.*, **75,** 691 (1976).

Salmon, R. "Two-layer quasi-geostrophic turbulence in a simple special case," *Geophys. Astrophys. Fluid Dynam.* **10,** 25 (1978).

Smagorinsky, J. "General circulation experiments with the primitive equations. I. The basic experiment," *Mon. Wea. Rev.*, **91,** 99 (1963).

Soong, T. T. *Random Differential Equations in Science and Engineering*. Academic Press, New York, 1973.

Stone, P. H. "Baroclinic adjustment," *J. Atmos. Sci.*, **35,** 561 (1978).